Title:

Salmonella injectisome penetration of macrophages triggers rapid translation of transcription factors and protection against cell death

Short title:

Salmonella injectisome interaction triggers rapid host translational induction

Authors

George Wood[a, §], Rebecca Johnson[a, §], Jessica Powell[a], Owain J. Bryant[a], Filip Lastovka[a], Matt Brember[a], Pani Tourlomousis[b], John P. Carr[c], Clare E. Bryant[b*] and Betty Y.W. Chung[a,*]

Affiliations

[a] Department of Pathology, University of Cambridge, Tennis Court Road, Cambridge, CB2 1QP, United Kingdom

[b] Department of Medicine and Department of Veterinary Medicine, University of Cambridge, Madingley Rd, Cambridge CB3 0ES, United Kingdom

[c] Department of Plant Sciences, University of Cambridge, Downing Street, Cambridge CB2 3EA, United Kingdom

[§] These authors contributed equally

Corresponding authors: ceb27@cam.ac.uk, bcy23@cam.ac.uk

'For the purpose of open access, the author has applied a Creative Commons Attribution (CC BY) licence to any Author Accepted Manuscript version arising'

Abstract

During bacterial infection both the host cell and its invader must divert intracellular resources to synthesise specific proteins in a timely manner. For the host, these factors may be needed for innate immune responses, including programmed cell death, and in the bacteria newly synthesized proteins may be survival factors needed to counteract host responses. *Salmonella* is an important food-borne bacterial pathogen that invades and multiplies within host cells. It is well established that invasion of epithelial cells is dependent upon the SPI-1 Type III injectisome, a biological needle that penetrates and secretes effectors into host cells to promote internalization. However, the importance of the SPI-1 injectisome in infection of professional phagocytes such as macrophages, which are the predominant host cell type

during systemic infection, is less clear. Through time resolved parallel transcriptomic and translatomic studies of macrophage infection, we revealed that SPI-1 injectisome-dependent infection of macrophages triggers rapid translation of transcription factor mRNAs, including Early Growth Response 1 (*Egr1*). Despite the short half-life of EGR1 protein, its swift synthesis within the initial hour of infection is sufficient to inhibit transcription of pro-inflammatory genes and thereby restrain inflammatory responses and programmed cell death within the first hour of during early infection. This transient period of inflammatory suppression in macrophages is exploited by *Salmonella* to establish infection and sheds new insight on the importance of translational activation in host-pathogen dynamics during *Salmonella* infection.

Introduction

The gene expression profiles of both host[1–5] and pathogen[6] are altered dramatically when they interact. This response is shaped by a co-evolutionary arms race where the host seeks to detect and counter the invading pathogen[3,5], whilst the pathogen aims to evade this response[6] and modify the host environment to better suit its survival and replication[1,2]. Changes in gene expression during infection are thus the net result of these competing goals, the balance of which can ultimately determine the infection outcome.

Many members of the Gram-negative bacterial genus *Salmonella* are facultative intracellular pathogens that infect a diverse spectrum of hosts. *Salmonella* species cause a range of diseases in humans, from typhoid fever to gastroenteritis. *Salmonella*'s ability to establish an intracellular infection is key to its pathogenesis[7]. During infection, the bacterium invades host cells, including the epithelial cells lining the intestinal tract and immune cells such as macrophages. Once internalized, *Salmonella* resides in a specialised membrane-bound compartment, the *Salmonella*-containing vacuole (SCV). The SCV provides a protective niche for the pathogen while giving it access to host cell nutrients to support its replication[8,9].

The intracellular lifestyle of pathogenic *Salmonella* is supported by two Type III secretion systems (T3SS) with different substrate specificity. The SPI-1 T3SS, also called the SPI-1 injectisome (hereafter, 'injectisome') is a multi-protein complex that spans the bacterial inner and outer membranes and cell wall, and transports proteins into target cells along a homomeric needle-like structure that is inserted into the host cell membrane by the bacterial effectors SipB, SipC and SipD[10–12]. PrgJ forms the inner rod that connects the injectisome basal body embedded in the *Salmonella* envelope with the needle structure and thus acts as a channel bridging the bacterial and host cytoplasms[10]. In epithelial cells, the injectisome is important in aiding host cell invasion via the trigger mechanism[13–15], though its role in establishing infection in professional phagocytes, such as macrophages, is less well

understood. The SPI-2 T3SS is expressed once the bacterium is internalized and supports the intracellular lifecycle of the pathogen[8,16].

To allow transport of effector proteins via the injectisome into the host cell, the *Salmonella* translocon subunits SipB and SipC are also secreted via the injectisome and inserted into the host cell plasma membrane to form a transient pore[11,12,17,18]. This insertion leads to transient loss of membrane integrity, therefore triggering an osmotic stress response and collapse of ion gradients with Ca^{2+} influx, and Cl^{-} and K^{+} efflux. Injectisome-dependent membrane damage is demonstrated by the haemolysin activity of the injectisome on red blood cells, which lyse upon SipBC insertion into their membranes[12]. While it is known that loss of membrane integrity, and the associated disruption of ion gradients, triggers inflammatory response pathways and cell death[17,19,20], the importance of this damage in eliciting host responses to *Salmonella* remains unclear.

In systemic infection, macrophages are the predominant host cell type and *Salmonella* survival in macrophages has been reported to be critical for virulence[7,21]. This is somewhat paradoxical given the importance of macrophages for the detection and elimination of pathogens[22]. Indeed, macrophages poses many receptors that detect *Salmonella* pathogen associated molecular patterns (PAMPs), which are crucial in controlling infection. This includes toll-like receptors (TLRs) such as TLR4 which detects bacterial lipopolysaccharide (LPS) on the *Salmonella* cell surface[23] as well as intracellular immune receptors that can activate the inflammasome and lead to inflammatory cell death[24–26]. In tissue culture, the majority macrophages die within the first few hour of infection[27–29] and this rapid cytotoxicity is dependent on the injectisome[27,29]. The balance between macrophage survival and death will influence the outcome of infection[22].

Although much research has been carried out on the transcriptional response of host cells to *Salmonella* infection[2–4], the analysis of gene expression is incomplete without also exploring regulation at the level of translation, i.e. protein synthesis. This is of particular importance given the critical nature of events occurring very early in infection. Translational regulation has the potential to allow for rapid responses, either through modulating translation of pre-existing mRNAs and/or by enhancing translation of the newly transcribed mRNAs. Indeed, previous studies have identified potent translational upregulation of inflammatory genes, such as *Tnf*, in macrophages following stimulation of TLR4 with purified LPS[30,31].

Here we utilized paired ribosome profiling and RNA-Seq over a time course of infection with wild type or SPI-1 injectisome mutant *Salmonella* in macrophages to understand the

110 dynamics of gene expression regulation throughout injectisome-dependent infection. We
111 identified that the translational response precedes the transcriptional response within sixty
112 min post infection, and it is enriched for genes that encode DNA binding proteins. Within the
113 translationally induced DNA binding proteins, we identified Early Growth Response 1 (*Egr1*).
114 *Egr1* showed rapid injectisome-dependent transcriptional induction, with even greater
115 translational induction, enabling the rapid and robust production of the EGR1 transcription
116 factor early in infection. We further demonstrated that, while the EGR1 protein turnover is
117 rapid, it acts as a longer term transcriptional suppressor of inflammatory genes triggered by
118 *Salmonella* infection. We hypothesise that this creates an early window of opportunity for
119 *Salmonella* to circumvent innate immunity, allowing it to successfully establish infection.
120

121 **Results**

122 ***Salmonella* infection triggers rapid host cell responses**

123 *Salmonella* entry into immortalized murine bone marrow derived macrophages (iBMDM,
124 hereafter 'macrophages' unless otherwise stated) is markedly enhanced by the injectisome,
125 although the mechanism in which it is involved in the invasion of professional phagocytes is
126 unclear[13–15,32]. *Salmonella* cells associated with host cell membrane, i.e. actively invading
127 bacteria, were seen as early as 5 min post-exposure, with *Salmonella* rapidly internalized
128 within 15 min (Figure 1A-B). There was little further macrophage infection after 15 min of
129 infection, indicating a potential change in susceptibility (Figure S1A). Injectisome-
130 independent internalization was assayed through infection with mutant *Salmonella* unable to
131 assemble the injectisome needle, generated by knockout of the SPI-1 inner-rod protein
132 PrgJ[33] and referred to as the 'injectisome mutant' hereafter. Invasion by injectisome mutant
133 *Salmonella* was also observable within this timeframe, though to a lesser degree than for
134 wildtype (WT) bacteria (Figure S1B).
135

136 As previously described[27–29], infection of macrophages with WT *Salmonella* led to rapid cell
137 death within the first 60 min of infection. However, approximately 25% of macrophages
138 survived despite the presence of viable intracellular bacteria (Figure 1C-D, S1A). In contrast,
139 and similar to previous studies[34], infection with injectisome mutant *Salmonella* did not induce
140 any increase in macrophage cell death (Figure 1D).
141

142 **Injectisome-dependent infection leads to both transcriptional and translational**
143 **induction of Early Growth Response 1 (EGR1) accumulation**

144 As a significant proportion of macrophages survive the lethal effect of injectisome
145 penetration (Figure 1A-D), we hypothesized that survival of infected cells beyond 60 min
146 post-infection with WT *Salmonella* may be a consequence of rapid gene expression

147 responses occurring within the first hour. This may be mediated by *de novo* transcription of
148 mRNAs, which has been the focus for most previous studies[2–4]. However, we suspected the
149 involvement of translational responses, which remain much less well understood, where the
150 rate of protein synthesis (translational efficiency) from mRNAs may be upregulated to
151 increase protein abundance more rapidly than could occur *via* transcription alone. Such an
152 acceleration of protein synthesis could be of critical importance given the short survival
153 timeframe of most infected cells. To investigate rapid transcriptional and translational
154 changes in gene expression, parallel global transcriptomic (RNA-Seq) and translatomic (i.e.,
155 ribosome profiling, Ribo-Seq hereafter) analyses were performed on macrophages at 60 min
156 following infection with either WT *Salmonella* or the injectisome mutant (Figure 1E, S1C).
157 Ribo-Seq is a highly sensitive method that reveals the global translatome at the time of
158 harvest[35]. The technique determines the position of ribosomes by exploiting the protection
159 from nuclease digestion of a discrete fragment of mRNA (~30 nucleotides) conferred by
160 elongating ribosomes. Deep sequencing of these ribosome-protected fragments (RPFs)
161 generates a high-resolution view of the location and abundance of translating ribosomes on
162 different mRNA species, reflecting the amount of synthesis of specific proteins (Figure 1E).
163 In addition, while RNA-Seq enables quantification of total mRNA abundance, parallel RNA-
164 Seq and Ribo-Seq enables quantification of translation efficiency, a measurement of how
165 well each mRNA is being translated as distinct from total protein synthesized (Figure 1F).
166
167 The resolution of our Ribo-Seq data is high, as evident from the metagene analysis
168 constructed with the software program riboSeqR[36]. The metagene translatome is a summed
169 plot of all translated mRNAs, with weighted average number of nucleotide reads around the
170 annotated coding start and stop sites, confirming accurate capture of the elongating
171 ribosome movement as almost all Ribo-Seq reads overwhelming maps to the first codon
172 position (S1C). This is further evidenced by our ability to directly visualize translation of
173 single genes at remarkable accuracy (Figure 1I), as well as non-canonical translation events.
174 For example, translation of *Atf4,* which is modulated by translation of two small upstream
175 open reading frames (uORFs) embedded within the 5'UTR of ATF4[37] (Figure S1E). The high-
176 resolution nature of our data therefore enables accurate quantification of protein synthesis
177 (i.e. total Ribo-Seq) and translational efficiency when combined with parallel RNA-Seq
178 (Figure 1F).
179
180 Initial analysis of macrophages infected by both WT and injectisome mutant *Salmonella*
181 identified many genes known to be upregulated upon exposure to bacterial PAMPs[30,31,38],
182 such as *Tnf* and *Zfp36*. These genes were upregulated not only in transcript abundance but
183 also at the translational level (Figure 1G, H, I and S1D and F). For both of these genes,

184 transcription was induced in response to either the WT or injectisome mutant *Salmonella*.
185 Potent translational upregulation was also seen, i.e. enhanced translational efficiency
186 resulting in greater protein synthesis than can be explained by an increase in *de novo* mRNA
187 synthesis alone (see Figure 1F), as has been previously reported in macrophages exposed
188 to purified bacterial LPS[30,31].
189
190 Following this, transcripts that were subject to specific injectisome-dependent translational
191 upregulation were investigated (Figure S1F). The key inflammasome component *Nlrp3* was
192 among the selectively induced genes (Figure S1G). The *Nlrp3* transcript has recently been
193 described to encode a uORF[39] which can be readily visualised in this data (Figure S1H). The
194 NLRP3 is activated in *Salmonella* infection but the uORF-mediated translational regulation of
195 *Nlrp3* is currently unclear[33,40,41]. To further identify injectisome-dependent translationally
196 regulated genes, transcripts where the $\log_2$ fold-change ($\log_2$FC) in translational efficiency
197 was greater than 1.5 in WT *Salmonella* infected macrophages over macrophages infected by
198 the injectisome mutant were selected (Figure 1J). Amongst the most translationally
199 upregulated mRNAs were those encoding Early Growth Response 1 (EGR1), NR4A1 and
200 Pro-Interleukin-1 beta (pro-IL-1β) (Figure 1J-K).
201
202 Interleukin-1 beta (IL-1β) is processed from its precursor pro-IL-1β into its mature, active
203 form by caspases; proteases that are themselves activated by the inflammasome[26,42]. This
204 precursor, encoded by *Il1b*, had a much greater translation efficiency in macrophages
205 infected by WT *Salmonella* than the injectisome mutant (Figure 1J-K). The injectisome is
206 known to transport bacterial effectors into the host cytosol that activate the inflammasome,
207 including components of the translocon such as SipB/C[43,44], consistent with our cytotoxicity
208 assay (Figure 1D), leading to IL-1β production[25,45]. These data suggest that IL-1β precursor
209 production is supported not only by increased mRNA transcription, but also post-
210 transcriptionally by specific upregulation of translation of its mRNA. Previous reports
211 describe the need for two signals to produce IL-1β: one to induce transcription of the
212 precursor and another to activate the inflammasome[43,46,47]. Importantly, however, our data
213 additionally reveal a strong role for translational upregulation in precursor production to
214 rapidly facilitate overall IL-1β precursor protein production. Therefore, the injectisome makes
215 an important contribution to macrophage pro-IL-1β production within the first 60 min, in
216 addition to delivering the factors that stimulate pro-IL-1β cleavage leading to IL-1β
217 production.
218
219 Both *Egr1* and *Nr4a1* are known immediate early genes that are rapidly transcribed in many
220 cell types within minutes in response to a range of cellular stresses[48–50]. Here we show that

while transcripts for both genes are almost absent in uninfected macrophages, rapid expression of these genes is enhanced by specific transcriptional upregulation leading to a surge of translational activation following injectisome-dependent infection (Figure 1J-K). NR4A1, also known as NUR77, is involved in macrophage responses to proinflammatory stimuli. NR4A1 limits inflammation in models of sepsis and colitis, likely through antagonism of the NF-κB pathway[51,52]. More recently, however, it has been reported to increase expression of proinflammatory cytokines in mice infected with *Klebsiella pneumoniae*[53]. The role of NR4A1 is therefore certainly immunomodulatory but likely differs by cell type and context.

Of the three transcripts chosen for detailed study, the most translationally induced is the mRNA for EGR1 (Figure 1J-K). EGR1 is a zinc-finger family transcription factor that binds GC-rich consensus sequences in gene promoters and enhancers, and it can either activate or suppress transcription. Targets of EGR1 span diverse biological processes including immune responses, cell growth and differentiation, and cell death[54–59]. Due to its highly injectisome-dependent translational upregulation, the biological function of EGR1 in *Salmonella*-macrophage infection was further characterized in this study.

Specific upregulation of EGR1 protein accumulation during the macrophage-*Salmonella* interaction is highly injectisome-dependent

Transcriptional upregulation of *Egr1* has previously been shown to be largely dependent on bacterial secretion systems in other infection contexts[2,60–62]. However, EGR1 has not been studied in the context of *Salmonella* infection of macrophages nor has post-transcriptional regulation of *Egr1* gene expression been studied. We were particularly interested in EGR1 given its association with cell death[54] and its importance in macrophage development[49,57].

At 60 min post-infection there was a clear increase in both transcription and translation of *Egr1* in WT-infected cells (Figure 1K, l and 2A). The increase in *Egr1* translation cannot be explained by the greater transcript abundance alone, but rather there is also an increase in *Egr1* mRNA translation efficiency. The translational efficiency of *Egr1* mRNA is three times higher in WT-infected cells compared to cells infected with the injectisome mutant (Figure 1K, l and 2A). In contrast, the *Egr1* expression in cells infected with the injectisome mutant were not much greater at 60 min post infection than in mock-infected cells. Reverse transcription-coupled quantitative PCR (RT-qPCR) for *Egr1* mRNA and immunoblot for EGR1 protein accumulation showed that during an infection time-course the upregulation was rapid but transient and that the half-lives of both *Egr1* mRNA and its protein product are short. While *Egr1* mRNA abundance peaked at 60 min and returned to baseline levels by

258 120 min (Figure 2B and C), the increase in protein abundance measured by immunoblotting
259 was, as expected, offset from the increase in mRNA, peaking at 120 min post-infection and
260 returning to undetectable levels by 240 min. The absence of EGR1 protein 240 min post-
261 infection indicates a short half-life for EGR1 protein and that its biological effect is likely rapid
262 (Figure 2C-D). In contrast, infection with the injectisome mutant led to a slight increase in
263 *Egr1* mRNA abundance at 60 min, followed by a detectable increase in EGR1 protein by 120
264 min, with both mRNA and protein at considerably lower levels than in WT *Salmonella*
265 infected cells (Figure 2A-D).
266
267 We reasoned that both *Egr1* transcriptional stimulation and the potent translational induction
268 (i.e. higher translational efficiency) could be either a result of the direct interaction of the
269 injectisome with macrophage, through insertion of the SipB/C translocon complex into the
270 macrophage plasmalemma[18], or due to transport of effector proteins once the injectisome is
271 fully assembled and is in a secretion competent state. To distinguish between these
272 possibilities, we engineered an injectisome blocking substrate in which the effector protein
273 SptP is C-terminally fused to the green fluorescent protein (SptP-GFP). This injectisome
274 blocking substrate is targeted to the export machinery and stalls within the injectisome
275 export channel because the folding of the GFP moiety (unlike the effector protein sequence)
276 is irreversible. Stalling occurs after needle assembly is complete, thereby blocking transport
277 of effectors and translocon subunits through the injectisomes that have assembled on the
278 bacterial cell surface[63], preventing penetration of macrophage plasmalemma (Figure 2E-F).
279 Obstructing the injectisome enabled us to uncouple the effect on *Egr1* upregulation upon
280 penetration of macrophage plasmalemma by the injectisome from transport of effector and
281 translocon subunits.
282
283 Expression of the SptP-GFP injectisome blocking substrate was controlled in the following
284 manner: (1) uninduced, therefore recapitulates WT infection where the injectisome
285 penetrates macrophages and delivers effectors; (2) Inducing expression of the blocking
286 substrate 2 h prior to macrophage infection, resulting in assembly of injectisomes that are
287 blocked with the SptP-GFP blocking substrate, preventing delivery of effectors whilst at the
288 same time preventing delivery and insertion of translocon subunits (SipB/SipC) into the host
289 cell membrane, which consequently abolishes penetration of macrophage plasmalemma;
290 and (3) blockage of injectisome induced at 5 min post-infection, therefore allowing
291 injectisomes to penetrate macrophage plasmalemma while inhibiting further delivery of
292 effectors (Figure 2E). As expected, transcription of *Egr1* was upregulated when
293 macrophages were infected by *Salmonella* with unobstructed injectisome (uninduced), but
294 expression is significantly impaired in macrophages challenged by *Salmonella* with a pre-

295 blocked, translocon-defective injectisome. However, *Egr1* transcript accumulation was only
296 slightly reduced when penetration of injectisome is established but delivery of effector is
297 prevented by SptP-GFP induction at 5 min post-infection (Figure 2G). Taken together, these
298 results suggest that the trigger for overall *Egr1* protein accumulation occurs very rapidly
299 during infection and is likely a direct result of injectisome penetration with the macrophage
300 plasmalemma or the action of the first few effector molecules that make it through the
301 injectisome.
302
303 **EGR1 protein restrains macrophage inflammatory responses to *Salmonella* infection**
304 To further investigate the role of EGR1 during injectisome dependent infection of
305 macrophages, we generated EGR1 knockout ($EGR1^{KO}$) macrophages using CRISPR-Cas9
306 and confirmed the absence of EGR1 protein 120 min after infection with WT *Salmonella*
307 (Figure 2H). Mutation of the *Egr1* coding sequence resulting in EGR1 knock-out in $EGR1^{KO}$
308 macrophages was confirmed through genomic DNA sequencing (Figure S2A). Loss of the
309 ability to produce EGR1 resulted in greater cell death at baseline, and this was further
310 increased when infected by WT *Salmonella*, particularly between 30 and 120 min post
311 infection (Figure 2I). This suggests EGR1 may play a role in limiting injectisome-induced
312 macrophage death. Following this, the role of EGR1 in the inflammatory response was
313 assessed by measuring the level of IL-1β produced by $EGR1^{KO}$ and $EGR1^{WT}$ macrophages
314 during infection. This revealed significantly greater upregulation in $EGR1^{KO}$ macrophages
315 infected with WT *Salmonella*, confirming that EGR1 has a suppressive role in the
316 inflammatory response.
317
318 As EGR1 is annotated as a DNA-binding protein, we hypothesized that EGR1 suppresses
319 inflammation through transcriptional regulation and so time-resolved transcriptomic analysis
320 (RNA-Seq) of WT *Salmonella*-infected $EGR1^{KO}$ or $EGR1^{WT}$ macrophages from 15 to 240 min
321 post infection was performed. Principal component analysis of gene transcript levels showed
322 a clear separation of samples by cell line and time post-infection. Principal component (PC)
323 1 largely reflects variation between the $EGR1^{KO}$ and $EGR1^{WT}$ cell lines, whereas PC2
324 separates the 120 min and 240 min infected samples from the 15 to 60 min infected samples
325 and 15 to 240 min mock inoculation treatments (Figure S2B). We observed a significant
326 increase in the abundance of transcripts associated with immune responses in the $EGR1^{KO}$
327 macrophages compared to the $EGR1^{WT}$ macrophages, particularly at 240 min post-infection,
328 confirming the suppression of transcription of inflammatory genes by EGR1 during
329 *Salmonella* infection (Figure 2K-L; Table S1-2). This includes *Il1b*, which showed greater
330 upregulation of transcription in $EGR1^{KO}$ macrophages infected with WT *Salmonella*. This is
331 likely the cause of the greater IL-1β secretion during *Salmonella* infection in the absence of

332 EGR1 (Figure 2J) and confirmed EGR1 as an important transcriptional immunomodulator. In
333 addition, gene ontology enrichment analysis also revealed significant upregulation of known
334 pro-cell death genes in infection of the EGR1^{KO} macrophages, including the FAS death
335 receptor, consistent with a role of EGR1 in limiting macrophage death (Figure 2L; Table S1-
336 2).
337
338 **The transcriptional and translational dynamics of Salmonella during macrophage**
339 **infection**
340 We have demonstrated that injectisome-dependent infection triggers surges both in *de novo*
341 mRNA synthesis and in translational efficiency of specific host mRNAs such as *Egr1*, leading
342 to rapid but transient accumulation of EGR1 protein. To assess global expression dynamics
343 throughout *Salmonella* infection, we therefore performed time-resolved parallel RNA-Seq
344 and Ribo-Seq of primary bone marrow-derived macrophages infected with WT *Salmonella* or
345 the injectisome mutant (Figure 3A). The use of primary macrophages (rather than the
346 iBMDMs used in previous experiments) allows us to compare injectisome- *versus* PAMP-
347 dependent responses in a system that more closely resembles *in vivo* infection. The primary
348 macrophages showed similar rates of infection to iBMDMs for WT *Salmonella*, but a greater
349 proportion were infected with the injectisome mutant compared to iBMDMs (Figure S1B and
350 S3A).
351
352 Due to the nature of the mRNA enrichment and library preparation method employed, both
353 host and bacterial translational and transcriptional dynamics were simultaneously captured
354 over the course of infection. Transcription and translation were also assessed in *Salmonella*
355 grown in Luria Broth (or lysogeny broth, LB) at various optical densities (OD). It has been
356 established that expression of SPI-1 in LB culture peaks at late exponential phase, OD 2[29],
357 as they were prepared for in these infection assays. This data demonstrates this increase in
358 expression of SPI-1 injectisome structural genes as the bacteria approach OD 2, through
359 enhanced translation (Figure 3B). Remarkably, we see significant transcriptional induction of
360 SPI-1 genes upon contact with macrophages, particularly structural components such as Prg
361 I/J and K, as early as 5-15 min. aligning with the timeframe of the initial Salmonella-
362 macrophage interaction (Figure 1A-C). This indicates that *Salmonella* respond to the
363 proximity of macrophages by upregulating expression of certain genes that enable invasion
364 (Figure 3B), and suggests that rapid assembly of injectisomes occurs on the bacterial cell
365 surface during the first 15 min. Indeed, the rapid assembly of additional T3SSs upon contact
366 with host cells has also been suggested in *Yersinia enterocolitica* infection[64]. The
367 transcriptional and translational response of non-structural SPI-1 genes that encode effector
368 proteins, structural genes with a dual-role as effectors such as *SipB* and *SipC*, and other

369 virulence factors also increased during the first 15 min whereas some genes, such as for
370 *AvrA* and *IacP*, were maximally expressed between 2-4 h post infection (Figure 3B).
371
372 Notably, during the early stages of infection (within the first 30 min), we also observed
373 increases in the translation efficiency of a subset of intramacrophage genes, including *htrA*,
374 *hisG* and *cpxP* (Figure 3B). Intramacrophage genes play a crucial role in the survival and
375 replication of the bacterium inside macrophages and in general maximal transcription for
376 these genes occurs later. The functions of these genes include roles in magnesium and
377 phosphate transport and the envelope stress response[65,66]. At the 30 min and 60 min time
378 points, when *Salmonella* is intracellular and after SCV acidification[67], the transcript
379 abundance of SPI-2 genes increases while the abundance of the majority of SPI-1
380 transcripts decreases (Figure 3B). This agrees with the recognized switch of *Salmonella*
381 secretion mediated by the transcriptional regulator SsrB. Concurrently we observed
382 decreases in expression of the flagella components, consistent with previously reported
383 SsrB-mediated repression[65,68,69] (Figure 3B).
384
385 **A global translational response precedes transcriptional responses in macrophages**
386 **following injectisome penetration.**
387 Analysis of parallel Ribo-Seq and RNA-Seq throughout the infection time course provided a
388 global perspective of the dynamics of host gene expression at multiple levels, notably
389 changes in RNA abundance and translation efficiency, by comparing primary macrophages
390 infected with either WT *Salmonella* or the injectisome mutant with mock infection (Figure
391 S4A). Within 5 min post infection, we can readily visualize that both WT and injectisome
392 mutant *Salmonella* induced rapid changes in translation efficiency of many genes compared
393 to mock, with more genes that are translationally induced in an injectisome-dependent
394 manner (Figure S4B). Furthermore, comparison of WT *Salmonella* and injectisome mutant
395 infections revealed that injectisome-specific translational upregulation precedes the
396 transcriptional regulation, with relatively little change in mRNA abundances within the first
397 120 min (Figure 3C-E). Many components of the classical inflammasome that are activated
398 by *Salmonella*[70], including *Nlrp3*, *Casp1* and *Gsdmd*, are among those transcriptionally
399 upregulated after 120 min of infection with either strain of *Salmonella* (Figure S4C). This is
400 after the initial wave of cell death (Figure 1C) that is typically attributed to inflammasome
401 activation.
402
403 Gene ontology enrichment analysis of transcripts with differential translational efficiencies
404 during the first 60 min of WT vs injectisome mutant *Salmonella* infection showed they have
405 functions related to cytokine activity and, strikingly, DNA binding and transcription (Figure 3F,

406 S4D, Table S3). In contrast, and similar to previous transcriptomic studies[3], the
407 transcriptional response was also enriched for cytokines and other cell signalling genes but
408 there was no such enrichment for DNA binding/transcription related genes. Beyond the initial
409 60 min, genes with injectisome-dependent transcriptional induction were enriched for DNA
410 binding functions, though the overlap with the rapidly transcriptionally regulated DNA binding
411 factors was small (Figure S4E). Overall, this reinforces the hypothesis that rapid,
412 injectisome-dependent translational induction of transcription modulators reshapes the
413 transcriptional landscape, and consequently, response of macrophages to *Salmonella*
414 infection.

415 **Discussion**

416 Cellular stress alters gene expression dynamics[1–5,71,72]. Here we show that bacterial infection
417 is a potent stressor that induces selective host protein synthesis through modulating mRNA
418 translation efficiency within the first hour of infection. Much of this regulation of translation
419 efficiency is rapidly triggered during the interaction between the *Salmonella* injectisome and
420 the macrophage plasmalemma, leading to the rapid synthesis of transcriptional modulators.
421 This appears to be triggered predominately by injectisome penetration, rather than the
422 subsequent injection of effector molecules. This study highlights the importance of cellular
423 responses to pathogen attack, and potentially other insults, to be able to rapidly generate
424 proteins, especially DNA binding proteins such as transcription factors, by modulating the
425 translation efficiency of mRNA molecules in the cytoplasm. This provides a mechanism to
426 synergize the transcriptional response to biotic stress.
427
428 We found that, in macrophages, one of the mRNAs controlled at the translational level
429 encoded the transcription factor EGR1. EGR1 induction was shown to negatively regulate
430 inflammation and cell death-associated genes resulting in enhanced cell survival and a
431 limited inflammatory response. EGR1 was recently found to be involved in macrophage
432 development by limiting the accessibility of inflammatory gene enhancers through
433 recruitment of the NuRD chromatin remodelling machinery[57] and is known to be rapidly and
434 transiently induced in response to various stimuli and has been assigned a diverse range of
435 roles, including regulating replication and cell death[54,58,59,73]. Here, we revealed that
436 accumulation of EGR1 protein is increased by a co-ordinated upregulation of translation as
437 well as transcription. Therefore, overall synthesis of EGR1 protein is particularly rapid and
438 robust and occurs within minutes after the bacterial injectisome interacts with the
439 macrophage plasmalemma. The *Egr1* mRNA and EGR1 protein levels both show tight
440 temporal control, with maximal levels at 60 and 120 min, respectively, declining to
441 undetectable levels within 4 h post-infection. This transient induction of EGR1 protein

442 actively contributes to macrophage survival, as supported by our infection study with the
443 EGR1^{KO} mutant. We subsequently revealed that EGR1 acts as a transcriptional suppressor
444 for genes associated with immune processes, including inflammatory genes such as IL-1β,
445 demonstrating the critical role of EGR1 in restraining the immune response during
446 *Salmonella* infection. Their increased expression likely contributes to the observed increases
447 in the rate of death of EGR1^{KO} mutant macrophages following infection. The rapid death of
448 *Salmonella*-infected macrophages is typically attributed to SPI-1[24,25]. Our data suggest that
449 EGR1 restrains pro-inflammatory signals in WT macrophages during *Salmonella* infection,
450 and thereby inhibits cell death[74,75]. While restraining inflammation likely contributes to
451 survival of macrophages, the decrease of pro-inflammatory and pro-cell death gene
452 expression due to transient EGR1 production appears to ultimately but inadvertently benefit
453 the bacterial invader as evidenced by the fact most macrophages that survive injectisome-
454 mediated infection continue to harbour viable bacteria intracellularly.
455
456 Our data obtained with *Salmonella* cells expressing the SptP-GFP blocking substrate to
457 inhibit T3SS-mediated effector secretion supports a model where *Egr1* upregulation at the
458 translational and transcriptional levels is triggered by penetration of the host cell membrane
459 by the bacterial injectisome. Recently, a model has been proposed that describes
460 transcriptional induction following exposure to the *Candida albicans* pore forming toxin
461 candidalysin[76]. We inferred that the injectisome-dependent translation and transcription of
462 *Egr1* is activated through a similar mechanism, as supported by observations that other
463 bacterial secretion systems require EGFR and ERK kinases for *Egr1* expression[60,62].
464 Supporting this, we show that induction of SPI-1-dependent *Egr1* expression occurs rapidly
465 as *Salmonella* establishes its infection, in the same timeframe as the T3SS is penetrating the
466 macrophages. We show that it is the penetration by the injectisome of the macrophage
467 plasmalemma that is responsible for increased EGR1 expression, not the secretion of
468 effectors.
469
470 In summary, we have demonstrated the significance of rapid, transient reprogramming of
471 gene expression, which is mediated primarily by increases in translation of mRNAs enriched
472 for DNA binding proteins. Many of these are transcription factors and will therefore
473 subsequently reshape the transcriptional landscape during the initial hour of *Salmonella*
474 infection of macrophages. Upon encountering host macrophages, *Salmonella* swiftly boosts
475 the expression of SPI-1 structural components, preparing for infection. Penetration of the
476 macrophage membrane by the SPI-1 injectisome is a major trigger for the changes in host
477 gene expression, which leads to rapid and robust protein production including that of EGR1.
478 EGR1 is a transcriptional suppressor of immune genes and therefore transient expression of

479 EGR1 restrains the inflammatory response and host cell death. We hypothesize that
480 *Salmonella* exploits this brief period of immunosuppression to establish infection, leading to
481 later downregulation of cytokine expression and host survival (Figure 4). In conclusion, this
482 work underscores the critical role of translational regulation in defining the response to
483 bacterial pathogens and the importance of Type III injectisome penetration of host cell
484 membranes, a neglected but crucial aspect of the host-bacterial interaction.

485 **Methods**

486 **Macrophage cell culture**

487 Primary bone marrow derived macrophages (BMDM) were harvested as previously
488 described[33]. Briefly, bone marrow from the rear legs of C57BL/6 mice was extracted,
489 suspended in culture media, and plated at a density of 10^6 cells/ml supplemented with
490 20 ng/ml M-CSF (Peprotech). Cells were differentiated for 7 days, with additional M-CSF
491 supplementation 4 days post-extraction. Immortalized bone marrow-derived macrophages
492 (iBMDM) were generated by retroviral transformation of bone marrow-derived macrophages
493 as previously described[77]. Cells were routinely grown in DMEM supplemented with 10%
494 foetal bovine serum at 37°C, 5% CO_2.
495

496 ***Salmonella* infection**

497 *Salmonella* Typhimurium SL1344 WT and Δ*prgJ* were sub-cultured in LB from stationary
498 phase cultures and grown at 37°C, with shaking at 200 rpm, until late exponential phase.
499 Bacteria were washed and diluted in culture media and added to cells at a multiplicity of
500 infection of 10. For infections using primary bone marrow-derived macrophages, all media
501 was supplemented with 20 ng/ml M-CSF. Unless otherwise indicated, after 15 min media
502 was supplemented with 100 µg/ml gentamicin.
503

504 **Microscopy**

505 At the indicated timepoint, cells were fixed in 4% paraformaldehyde, permeabilized and
506 stained with Phalloidin-CF594 conjugate (Biotium), and goat anti-*Salmonella* CSA-1 (Insight
507 Biotechnology) followed by anti-goat IgG conjugated to Alexa488 (Abcam). Cells were
508 imaged and the proportion infected determined. Macrophages with intracellular bacteria, as
509 determined by the intensity of CSA-1 staining and the position of *Salmonella* within the cell,
510 were considered infected. Macrophages that were uninfected (no intracellular bacteria) but
511 had *Salmonella* associated with the host cell surface membrane were considered to be in
512 the process of becoming infected.
513

514 **Gentamicin protection assay**

515 The use of gentamicin protection assay to assess the number of intracellular bacterial has
516 been described previously[2]. This protocol was modified to better account for host cell death.
517 Briefly, 1 h post gentamicin treatment (i.e. 75 min post infection) macrophages were
518 trypsinized, counted, and lysed in 0.09% Triton X-100. Serial dilutions of lysates were plated
519 on LB-agar and grown at 37°C overnight. The *Salmonella* colonies were counted and divided
520 by the number of counted host macrophages.
521
522 **Cytotoxicity assay**
523 Cytotoxicity was measured by lactate dehydrogenase release using the CytoTox 96 Non-
524 Radioactive Cytotoxicity Assay kit (Promega) according to the manufacturer's instructions.
525 Cytotoxicity was determined relative to total cell lysis by 0.9% Triton X-100.
526
527 **Ribosome profiling with parallel RNA sequencing**
528 Ribosome profiling was performed as previously described[36], a schematic of which is
529 presented in Figure 1E. Briefly, at the indicated timepoint, culture supernatant was removed
530 from cells and flash frozen. Cells were lysed in buffer containing cycloheximide and
531 chloramphenicol, and lysates were split for RNA-Seq and Ribo-Seq. For Ribo-Seq, lysates
532 were treated with RNase I and fragments protected from digestion by the ribosome were
533 purified. For RNA-Seq, total cellular RNA was fragmented by alkaline hydrolysis. This was
534 followed by library generation as previously described[36,78–80] . Sequencing was performed
535 using NextSeq-500 or 2000 (Illumina).
536
537 Reads were aligned sequentially to mouse rRNA, mouse mRNA, *Salmonella* rRNA and
538 *Salmonella* mRNA. Mouse reference sequences were based on NCBI release mm10, and
539 *Salmonella* reference sequences were based on GenBank sequences FQ312003.1,
540 HE654725.1, HE654726.1 and HE654724.1. RiboSeqR[36] was used to confirm the quality of
541 libraries and to count reads aligning to coding sequences. Xtail[81] was used to determine
542 differential translational efficiency of these coding sequences and edgeR[82] was used for
543 normalization and to filter *Salmonella* genes by expression for retention in further analysis.
544 Gene set enrichment analysis was performed using g:Profiler[83].
545
546 **Western immunoblotting**
547 Protein was harvested from cells disrupted with lysis buffer (50 mM Tris-HCl pH 8.0, 150 mM
548 NaCl, 1 mM EDTA, 10% glycerol, 1% Triton X-100, 0.1% IGEPAL-CA630) containing
549 protease (cOmplete Mini, Roche) and phosphatase inhibitors (PhosSTOP, Roche). 30 µg
550 protein was separated by SDS-PAGE and transferred to nitrocellulose membrane. EGR1
551 was detected using rabbit anti-EGR1 (Cell Signaling) followed by anti-rabbit conjugated to

552 HRP (Cell Signaling). The HRP signal was assayed using SuperSignal West Pico PLUS
553 substrate (Thermo Scientific). GAPDH was detected using mouse anti-GAPDH (Sigma
554 Aldrich) followed by anti-mouse conjugated to IRDye 800 CW (Licor). SipC was detected by
555 mouse anti-SipC (tgcBIOMICS) followed by anti-mouse IgG antibody conjugated to HRP
556 (Promega). GroEL was detected by rabbit anti-GroEL (Abcam) followed by anti-rabbit IgG
557 antibody conjugated to HRP (Promega). Myc tagged SptP-GFP blocking substrates were
558 detected with anti-Myc-HRP conjugate mouse antibody (Cell Signaling).
559
560 **Reverse transcription quantitative polymerase chain reaction (RT-qPCR)**
561 RNA was extracted from cells using TRIzol (Invitrogen) per the manufacturer's instructions.
562 Reverse transcription was performed using M-MLV reverse transcriptase (Promega) with
563 random hexamer primers 'Promega) per the manufacturer's instructions. Realtime qPCR
564 was performed using iTaq Universal SYBR Green Supermix (Bio-Rad) and assayed on ViiA
565 7 system (Applied Biosystems) per the manufacturer's instructions. Primers were designed
566 using PrimerBLAST (Table S4).
567
568 **Knockout of EGR1**
569 The Alt-R CRISPR-Cas system (IDT) was used per the manufactures instructions to edit the
570 *Egr1* coding sequence using guide RNAs targeting *Egr1* or no genes as a negative control
571 (Table S5)[84]. The system was delivered by lipofection into macrophages using Lipofectamine
572 CRISPRMAX (Invitrogen). A clonal population was generated and targeted Sanger
573 sequencing at the *Egr1* locus was performed (Genewiz) to confirm mutation of *Egr1*.
574
575 **Blocked injectisome *Salmonella* transformant**
576 Type III injectisomes can be blocked by fusing GFP to the C-terminus of an effector protein[63].
577 To generate our inducible blocking substrate construct, gDNA encoding the *Salmonella*
578 chaperone SicP (residues 1-116) up to and including the downstream gene encoding the
579 effector protein SptP (residues 1-543) was inserted into the pTrc99a plasmid[85] in-frame with
580 sequence encoding C-terminal GFP followed by a myc-tag. IPTG induction results in the
581 production of an mRNA transcript encoding wild type SicP chaperone which promotes
582 efficient targeting of SicP's cognate substrate (in this case the SptP-GFP-myc blocking
583 substrate) to the injectisome export machinery. The mRNA transcript also encodes the SptP-
584 GFP-myc fusion protein which is targeted to the injectisome export machinery and stalls
585 within the export channel, blocking the secretion of effector proteins via the SPI-1
586 injectisome. To block effector protein secretion via the injectisome, *Salmonella* cells carrying
587 the inducible blocking substrate construct were grow in LB containing 100 µg.ml ampicillin
588 and expression of the blocking substrate (and the SicP chaperone) was achieved by

589 supplementing the media with isopropyl β-D-1-thiogalactopyranoside (IPTG) to a final
590 concentration of 100 μM.

591

592 **mRNA 3' end sequencing**

593 Preparation of mRNA 3' end sequencing libraries was performed using QuantSeq 3' mRNA-
594 Seq Library Prep Kit (Lexogen) with TRIzol extracted RNA and libraries were sequenced by
595 Novogene Ltd. Reads were aligned to the mouse genome (mm10) and those aligning to
596 genes counted. Read count normalization and differential expression analysis was
597 performed using edgeR.

598

599 **Enzyme-linked immunosorbent assay (ELISA)**

600 Culture supernatants were removed from infected cells at the indicated timepoint. ELISAs
601 were performed to quantify IL-1β in these culture supernatants using the Mouse IL-1 beta/IL-
602 1F2 DuoSet ELISA kit (R&D Systems) per the manufacturer's instructions.

603

604 **Protein export assays**

605 Export assays were performed as previously described[86]. Briefly, *Salmonella* strains were
606 cultured at 37 °C in LB broth with 100 μM IPTG to mid-log phase (OD600nm 1.5) for 2 h.
607 Cells were centrifuged (6000 x g, 3 min) and resuspended in fresh media and grown for a
608 further 60 min at 37 °C. The cells were pelleted by centrifugation (16,000 x g, 5 min) and the
609 supernatant passed through a 0.2 μm nitrocellulose filter. Proteins were precipitated with
610 10% trichloroacetic acid (TCA) and 1% Triton X-100 on ice for 1 hr, pelleted by centrifugation
611 (16,000 x g, 10 min), washed with ice-cold acetone, and resuspended in SDS-PAGE loading
612 buffer (volumes calibrated according to cell densities). Fractions were analyzed by
613 immunoblotting with anti-SipC (tgcBIOMICS), anti-Myc (Cell Signaling) and anti-GroEL
614 (Abcam) anti-sera.

615

616 **Data availability.**

617 Raw and processed data are available from ArrayExpress accessions E-MTAB-13212 and
618 E-MTAB-13213 or can be found in the supplementary tables. Customized scripts used for
619 this project are available upon request.

620

621 **Conflict of interest:**

622 The authors declare no conflict of interest

623

Acknowledgements:

We would also like to thank Jim Kaufman, Klaus Okkenhaug, and Alex Murphy for discussions and comments on the manuscript. F.L. was supported by a BBSRC DTP studentship. G.W. was supported by the Department of Pathology PhD studentship, B.Y.W.C., R.J. and M.B. and O.J.B. are supported by a Medical Research Council Fellowship to B.Y.W.C. [MR/R021821/1]. J.P. and M.B. are supported by a BBSRC project grant awarded to B.Y.W.C. [BB/V006096/1]. The B.Y.W.C. laboratory is supported by a Medical Research Council Fellowship [MR/R021821/1], BBSRC project grants [BB/X001261/1, BB/V017780/1 and BB/V006096/1] and a Royal Society Research Grant [RGS\R2\192222]. Figures created with BioRender.com.

Author contributions:

B.Y.W.C. conceived the research. B.Y.W.C., G.W., R.J., J.P., O.J.B., F.L., J.P.C. and C.B. designed experiments. R.J., J.P. and B.Y.W.C. generated RiboSeq, RNA-Seq and QuantSeq libraries. G.W., R.J. and J.P. performed molecular and cell biology experiments. O.J.B. generated *Salmonella* mutants. F.L. performed bacterial bioinformatics. B.Y.W.C., G.W., R.J., J.P., F.L. and M.B. performed the bioinformatic analysis. C.B. provided macrophages and *prgJ* mutant. P.T. provided training for extracting BMDM. B.Y.W.C., G.W., O.J.B. and J.P.C. wrote the manuscript.

Figure Legends

Fig 1: *Salmonella* SPI-1 dependent infection rapidly alters macrophage translation. (**A**) Mock infected and WT *Salmonella* infected macrophages 5 min post infection. Actin is shown in red, and *Salmonella* are shown in green. Arrows indicate *Salmonella* associated with the cell membrane. (**B**) Percentage of macrophages affected by WT *Salmonella* during the first 15 min of infection determined by immunofluorescent microscopy. Infected cells contain intracellular *Salmonella* infecting cells do not but have *Salmonella* associated with the host cell membrane, *n*=3. (**C**) *Salmonella* colony forming units (CFU) recovered 75 min post WT and SPI-1 deficient (Δ*prgJ*) *Salmonella* infection per host macrophage. Significance determined by Student's t-test; *n*=2. (**D**) Cytotoxicity of WT or Δ*prgJ Salmonella* or mock infection of macrophages as determined by lactate dehydrogenase (LDH) release into culture supernatant. Significance determined by Students t-test; *n*=2. (**E**) Experimental outline detailing the preparation of ribosome profiling and RNA-Seq libraries from infected macrophages. Details are provided in the materials and methods (RPF: ribosome-protected RNA fragments, NGS: next-generation sequencing). (**F**) Diagram illustrating the relationship between mRNA abundance (measured by RNA-Seq), protein synthesis (measured by Ribo-

660 Seq) and translational efficiency (TE). (**G**) Comparison of changes in mRNA abundance (left)
661 and TE (right) on infection with WT or Δ*prgJ Salmonella* over mock infection. Genes
662 upregulated transcriptionally in both ($log_2FC > 1$) are shown in red. (**H**) Heatmap showing
663 mRNA abundance, protein synthesis and TE of transcriptionally upregulated genes
664 highlighted in G. Genes are ordered by hierarchical clustering of mRNA abundance across
665 all conditions (left) (**I**) Ribo-Seq and RNA-Seq coverage of *Tnf* and *Zfp36* transcripts, which
666 are known to have increased TE on exposure to bacterial PAMPs. Ribo-Seq reads are
667 represented by their P site position and colored by their reading frame relative to the start
668 codon of the coding sequence, represented by the bar above each plot with the start and
669 stop positions indicated on the x-axis. *Rpl4* is presented as a control gene expressed in all
670 samples. Significance determined using Xtail as described in the Materials and Methods (**J**)
671 Normalized mRNA abundance, protein synthesis and TE of genes with log_2FC in TE of WT
672 over Δ*prgJ* infected macrophages greater than 1.5 and at least 50 normalized Ribo-Seq
673 counts in WT infection. Genes are ordered by hierarchical clustering of TE across all
674 conditions (left). Genes with low read counts (i.e. those with normalized RNA-Seq and Ribo-
675 Seq counts less than 5) are considered lowly expressed and therefore TE cannot be reliably
676 calculated. (**K**) Ribo-Seq and RNA-Seq transcript coverage of *Egr1*, *Il1b* and *Nr4a1* as in **G**.
677
678 **Fig 2**: *Egr1* is rapidly induced in *Salmonella* infection to restrict expression of immune
679 response genes. (**A**) mRNA abundance, protein synthesis and translational efficiency (TE) of
680 *Egr1* from Fig 1K. For conditions with low *Egr1* expression TE cannot be reliably calculated
681 (grey bar); significance determined using Xtail as described in the Materials and Methods.
682 (**B**) *Egr1* transcript abundance over WT and SPI-1 deficient mutant (Δ*prgJ*) infection,
683 normalized to the housekeeping gene *Supt16* and relative to cells prior to infection, *n*=2. (**C**)
684 Quantification of EGR1 abundance from **D** normalized to GAPDH. (**D**) Immunoblot following
685 EGR1 and GAPDH protein abundance across WT and Δ*prgJ* infection. An equal amount of
686 cellular protein was loaded per lane. (**E**) Experimental outline illustrating the effect of the
687 SptP-GFP injectisome blocking substrate on protein export via the injectisome. *Salmonella*
688 cells not producing the blocking substrate can transport effector proteins into host cells
689 (unobstructed injectisome, left). *Salmonella* cells expressing the injectisome blocking
690 substrate before infection are unable to transport effector subunits via the injectisome (pre-
691 blocked injectisome, middle). *Salmonella* cells were also incubated with macrophages for 5
692 min before inducing expression of the injectisome blocking substrate such that injectisomes
693 can engage with macrophage cells but secretion of effectors proteins from *Salmonella* into
694 macrophages are blocked at 5 min (injectisome blocked at 5 min, right). (**F**) Secretion
695 analysis of WT *Salmonella* either expressing the SptP-GFP injectisome blocking subunit or
696 carrying empty vector. Whole cell (cell) and secreted proteins (sec) from late-exponential-

phase cultures were separated by SDS-PAGE and immunoblotted with anti-Myc-tag (SptP-GFP), anti-SipC or anti-GroEL antisera. (**G**) *Egr1* transcript abundance over the *Salmonella* infection time course with blockade of the SPI-1 injectisome induced at various timepoints. Significance determined by one-sided Student's t-test; *n*=2. (**H**) Immunoblot showing EGR1 expression in $EGR1^{WT}$ and $EGR1^{KO}$ macrophages infected with WT *Salmonella* at 120 min post infection. (**I**) Cytotoxicity of WT or mock infection of $EGR1^{WT}$ and $EGR1^{KO}$ macrophages as determined by lactate dehydrogenase (LDH) release into culture supernatant. (**J**) IL-1β concentration in culture supernatant from infected $EGR1^{KO}$ and $EGR1^{WT}$ macrophages. *n*=2 except for 240 min WT *Salmonella* infection where n=3 for $EGR1^{WT}$ and 4 for $EGR1^{KO}$; significance determined using one-sided Student's t-test. (**K**) Normalized mRNA abundance of transcripts upregulated ($log_2FC > 2$) in $EGR1^{KO}$ when compared to $EGR1^{WT}$ macrophages at any timepoint in WT *Salmonella* infection. Genes are ordered by hierarchical clustering (left). (**L**) The 10 most significantly enriched gene ontology biological process terms in genes identified in J.

Fig 3: Time resolved RiboSeq reveals dynamic changes in host and bacterial translation. Data from two replicates. (**A**) Outline of infection time course. Primary bone marrow-derived macrophages were generated from mice and infected with WT or Δ*prgJ* mutant *Salmonella*. Gentamicin was used to kill extracellular bacteria at 15 min and its concentration was reduced after 1 h. (**B**) Transient expression dynamics of select WT *Salmonella* genes at different optical densities (OD) and over 4 h of macrophage infection, at the level of mRNA abundance, protein synthesis and translation efficiency. (**C**) Differential regulation of host gene expression as measured by the log_2FC of translational efficiency (TE) vs log_2FC mRNA abundance in WT *Salmonella* infection over Δ*prgJ* infection. Dashed orange lines show the log_2FC cutoffs (±2) used to select differentially expressed genes, and genes that pass these thresholds are colored. Only genes with log_2FC in mRNA and TE between -5 and 5 are shown here (see Fig S4B for uncropped plots). (**D** and **E**) Number of genes differentially expressed between WT and Δ*prgJ Salmonella* infection at both the TE (**D**) and mRNA (**E**) levels. (**F**) Top 10 enriched GO molecular function terms in differentially expressed genes at both the TE (right) and mRNA (left) levels. Genes were split by when they were differentially expressed: at or before 60 min, and after 60 min post infection.

Fig 4: Summary and model. Specific classes of *Salmonella* genes are transiently expressed as infection is established, including rapid upregulation of SPI-1 genes as bacteria encounter host macrophages, leading to increased production of T3SS injectisomes as shown. *Salmonella* SPI-1 injectisome assembly forms transient pores in the host membrane which activates host signaling pathways, leading to increased *Egr1* transcription and enhanced

translation. EGR1 negatively modulates immune gene transcription and, in doing so, inflammatory cytokine production in response to *Salmonella* infection is restrained, as is host cell death.

Fig S1: (**A**) Percentage of macrophages infected by WT *Salmonella* determined by microscopy at 15 and 60 min, with and without addition of gentamicin at 15 min. Significance determined by Student's t-test; *n*=2. (**B**) Percentage of macrophages infected by WT or Δ*prgJ Salmonella* determined by microscopy at 15 min. Significance determined by Student's t-test; *n*=2. (**C**) Meta-gene translatome from ribosome profiling of *Salmonella* infected macrophages at 60 min. Histograms of RPF 5′ ends relative to start and stop codons colored by their reading frame relative to the coding sequence. (**D**) Heatmap showing mRNA abundance, protein synthesis and TE of all genes in Fig 1G. Genes are ordered by hierarchical clustering of mRNA abundance across all conditions (left). Arrows indicate direction of differential transcript abundance ($\log_2$FC ±1) in the indicated infection vs mock.
(**E**) Ribo-Seq and RNA-Seq transcript coverage of *Atf4*. Ribo-Seq reads are represented by their P site position and colored by their reading frame relative to the start codon of the main *Atf3* coding sequence. Open reading frames are represented by bars above each plot. (**F**) Comparison of changes in mRNA abundance (left) and TE (right) on infection with WT over mock infection or Δ*prgJ Salmonella*. Genes upregulated transcriptionally in both ($\log_2$FC > 1) are shown in red. *Egr1*, *Nr4a1* and *Nfkbiz* are plotted separately due to low abundance in mock infection precluding accurate calculation of TE, and as such TE fold change in WT *Salmonella* over mock infection. (**F**) Normalised mRNA abundance and protein synthesis of *Nlrp3* at 60 min post-infection. (**G**) Ribo-Seq and RNA-Seq transcript coverage of *Nlrp3* as in **E**. The *Nlrp3* uORF can be readily seen as reads in a different reading frame within the 5' UTR.

Fig S2: (**A**) Example section of the *Egr1* coding sequence with an alignment from targeted sequencing of the Egr1 locus in the EGR1 KO macrophages. Mismatched bases and deletions are highlighted in red. (**B**) Principal component analysis of the transcriptomes of WT *Salmonella* infected or mock infected EGR1 KO or control macrophages over an infection time course.

Fig S3: (**A**) Percentage of primary macrophages infected by WT or Δ*prgJ Salmonella* determined by microscopy at 15 min. (**B**) Meta-gene translatome from ribosome profiling across a *Salmonella* primary bone marrow derived macrophage infection time course.

770 Histograms of RPF 5′ ends relative to start and stop codons colored by their reading frame
771 relative to the coding sequence.
772
773 **Fig S4**: (**A**) log_2FC TE vs log_2FC mRNA abundance between the indicated infections, across
774 the time course. Dashed orange lines show the log_2FC cutoffs (±2) used to select
775 differentially expressed genes; genes that pass these thresholds are colored. (**B**) Number of
776 genes differentially expressed between WT vs mock and Δ*prgJ* vs mock infection at both the
777 TE (right) and mRNA (left) levels. (**C**) Expression of genes encoding components of the
778 inflammasome[70] that are upregulated over the infection timecourse. (**D**) Top 10 enriched GO
779 molecular function terms in differentially expressed genes at both the TE (right) and mRNA
780 (left) levels. Genes were split by when they were differentially expressed: at or before 60
781 min, and after 60 min post infection. (**E**) Overlap of genes with DNA binding and transcription
782 related annotations that are differentially regulated on the translational level at or before 60
783 min or the transcriptional level after 60 min in the comparison of WT vs Δ*prgJ* infection.
784

785 **References**

786 1. Denzer, L., Schroten, H., and Schwerk, C. (2020). From gene to protein - how
787 bacterial virulence factors manipulate host gene expression during infection. Int. J.
788 Mol. Sci. *21*, 3730. 10.3390/ijms21103730.

789 2. Hannemann, S., Gao, B., and Galán, J.E. (2013). Salmonella modulation of host cell
790 gene expression promotes its intracellular growth. PLoS Pathog. *9*, e1003668.
791 10.1371/journal.ppat.1003668.

792 3. Jensen, K., Gallagher, I.J., Kaliszewska, A., Zhang, C., Abejide, O., Gallagher, M.P.,
793 Werling, D., and Glass, E.J. (2016). Live and inactivated Salmonella enterica serovar
794 Typhimurium stimulate similar but distinct transcriptome profiles in bovine
795 macrophages and dendritic cells. Vet. Res. *47*. 10.1186/s13567-016-0328-y.

796 4. Ordas, A., Hegedus, Z., Henkel, C. V, Stockhammer, O.W., Butler, D., Jansen, H.J.,
797 Racz, P., Mink, M., Spaink, H.P., and Meijer, A.H. (2011). Deep sequencing of the
798 innate immune transcriptomic response of zebrafish embryos to Salmonella infection.
799 Fish Shellfish Immunol. *31*, 716–724. 10.1016/j.fsi.2010.08.022.

800 5. Maekawa, S., Wang, P.C., and Chen, S.C. (2019). Comparative study of immune
801 reaction against bacterial infection from transcriptome analysis. Front. Immunol. *10*.
802 10.3389/fimmu.2019.00153.

803 6. Westermann, A.J., Venturini, E., Sellin, M.E., Förstner, K.U., Hardt, W.D., and Vogel,
804 J. (2019). The major RNA-binding protein ProQ impacts virulence gene expression in

805 Salmonella enterica serovar Typhimurium. MBio *10*, e02504-2518.
806 10.1128/mBio.02504-18.

807 7. Fields, P.I., Swanson, R. V., Haidaris, C.G., and Heffron, F. (1986). Mutants of
808 Salmonella Typhimurium that cannot survive within the macrophage are avirulent.
809 PNAS *83*, 5189–5193. 10.1073/pnas.83.14.5189.

810 8. Liss, V., Swart, A.L., Kehl, A., Hermanns, N., Zhang, Y., Chikkaballi, D., Böhles, N.,
811 Deiwick, J., and Hensel, M. (2017). Salmonella enterica remodels the host cell
812 endosomal system for efficient intravacuolar nutrition. Cell Host Microbe *21*, 390–402.
813 10.1016/j.chom.2017.02.005.

814 9. Jiang, L., Wang, P., Song, X., Zhang, H., Ma, S., Wang, J., Li, W., Lv, R., Liu, X., Ma,
815 S., et al. (2021). Salmonella Typhimurium reprograms macrophage metabolism via
816 T3SS effector SopE2 to promote intracellular replication and virulence. Nat. Commun.
817 *12*, 1–18. 10.1038/s41467-021-21186-4.

818 10. Miletic, S., Fahrenkamp, D., Goessweiner-Mohr, N., Wald, J., Pantel, M., Vesper, O.,
819 Kotov, V., and Marlovits, T.C. (2021). Substrate-engaged type III secretion system
820 structures reveal gating mechanism for unfolded protein translocation. Nat. Commun.
821 *12*, 1546. 10.1038/s41467-021-21143-1.

822 11. Myeni, S.K., Wang, L., and Zhou, D. (2013). SipB-SipC complex is essential for
823 translocon formation. PLoS One *8*, e60499. 10.1371/journal.pone.0060499.

824 12. Miki, T., Okada, N., Shimada, Y., and Danbara, H. (2004). Characterization of
825 Salmonella pathogenicity island 1 type III secretion-dependent hemolytic activity in
826 Salmonella enterica serovar Typhimurium. Microb. Pathog. *37*, 65–72.
827 10.1016/j.micpath.2004.04.006.

828 13. Ly, K.T., and Casanova, J.E. (2007). Mechanisms of Salmonella entry into host cells.
829 Cell. Microbiol. *9*, 2103–2111. 10.1111/j.1462-5822.2007.00992.x.

830 14. Galán, J.E. (1998). Interactions of Salmonella with host cells: Encounters of the
831 closest kind. Proc. Natl. Acad. Sci. *95*, 14006–14008. 10.1073/pnas.95.24.14006.

832 15. Hume, P.J., Singh, V., Davidson, A.C., and Koronakis, V. (2017). Swiss army
833 pathogen: The Salmonella entry toolkit. Front. Cell. Infect. Microbiol. *7*, 348.
834 10.3389/fcimb.2017.00348.

835 16. Vazquez-Torres, A., Xu, Y., Jones-Carson, J., Holden, D.W., Lucia, S.M., Dinauer,
836 M.C., Mastroeni, P., and Fang, F.C. (2000). Salmonella Pathogenicity Island 2-
837 Dependent Evasion of the Phagocyte NADPH Oxidase. Science (80-.). *287*, 1655–

838 1658. 10.1126/science.287.5458.1655.

839 17. Guignot, J., and Tran Van Nhieu, G. (2016). Bacterial control of pores induced by the
840 type III secretion system: mind the gap. Front. Immunol. *7*, 84.
841 10.3389/fimmu.2016.00084.

842 18. Park, D., Lara-Tejero, M., Waxham, M.N., Li, W., Hu, B., Galán, J.E., and Liu, J.
843 (2018). Visualization of the type III secretion mediated salmonella–host cell interface
844 using cryo-electron tomography. Elife *7*. 10.7554/ELIFE.39514.

845 19. Murthy, S., Karkossa, I., Schmidt, C., Hoffmann, A., Hagemann, T., Rothe, K., Seifert,
846 O., Anderegg, U., von Bergen, M., Schubert, K., et al. (2022). Danger signal
847 extracellular calcium initiates differentiation of monocytes into SPP1/osteopontin-
848 producing macrophages. Cell Death Dis. 2022 131 *13*, 1–15. 10.1038/s41419-022-
849 04507-3.

850 20. Koumangoye, R. (2022). The role of Cl-and K+efflux in NLRP3 inflammasome and
851 innate immune response activation. Am. J. Physiol. - Cell Physiol. *322*, C645–C652.
852 10.1152/AJPCELL.00421.2021/ASSET/IMAGES/LARGE/AJPCELL.00421.2021_F00
853 2.JPEG.

854 21. Richter-Dahlfors, A., Buchan, A.M.J., and Finlay, B.B. (1997). Murine salmonellosis
855 studied by confocal microscopy: Salmonella Typhimurium resides intracellularly inside
856 macrophages and exerts a cytotoxic effect on phagocytes in vivo. J. Exp. Med. *186*,
857 569–580. 10.1084/jem.186.4.569.

858 22. Price, J. V., and Vance, R.E. (2014). The macrophage paradox. Immunity *41*, 685–
859 693. 10.1016/j.immuni.2014.10.015.

860 23. Talbot, S., Tötemeyer, S., Yamamoto, M., Akira, S., Hughes, K., Gray, D., Barr, T.,
861 Mastroeni, P., Maskell, D.J., and Bryant, C.E. (2009). Toll-like receptor 4 signalling
862 through MyD88 is essential to control Salmonella enterica serovar Typhimurium
863 infection, but not for the initiation of bacterial clearance. Immunology *128*, 472.
864 10.1111/J.1365-2567.2009.03146.X.

865 24. Grant, A.J., Sheppard, M., Deardon, R., Brown, S.P., Foster, G., Bryant, C.E.,
866 Maskell, D.J., and Mastroeni, P. (2008). Caspase-3-dependent phagocyte death
867 during systemic Salmonella enterica serovar Typhimurium infection of mice.
868 Immunology *125*, 28–37. 10.1111/j.1365-2567.2008.02814.x.

869 25. Gram, A.M., Wright, J.A., Pickering, R.J., Lam, N.L., Booty, L.M., Webster, S.J., and
870 Bryant, C.E. (2021). Salmonella flagellin activates NAIP/NLRC4 and canonical NLRP3
871 inflammasomes in human macrophages. J. Immunol. *206*, 631–640.

872 10.4049/jimmunol.2000382.

873 26. Bergsbaken, T., Fink, S.L., and Cookson, B.T. (2009). Pyroptosis: host cell death and
874 inflammation. Nat. Rev. Microbiol. *7*, 99–109. 10.1038/nrmicro2070.

875 27. Chen, L.M., Kaniga, K., and Galán, J.E. (1996). Salmonella spp. are cytotoxic for
876 cultured macrophages. Mol. Microbiol. *21*, 1101–1115. 10.1046/j.1365-
877 2958.1996.471410.x.

878 28. Monack, D.M., Raupach, B., Hromockyj, A.E., and Falkow, S. (1996). Salmonella
879 Typhimurium invasion induces apoptosis in infected macrophages. PNAS *93*, 9833–
880 9838. 10.1073/pnas.93.18.9833.

881 29. Lundberg, U., Vinatzer, U., Berdnik, D., von Gabain, A., and Baccarini, M. (1999).
882 Growth phase-regulated induction of Salmonella-induced macrophage apoptosis
883 correlates with transient expression of SPI-1 genes. J. Bacteriol. *181*, 3433–3437.
884 10.1128/JB.181.11.3433-3437.1999.

885 30. Wang, L., Trebicka, E., Fu, Y., Waggoner, L., Akira, S., Fitzgerald, K.A., Kagan, J.C.,
886 and Cherayil, B.J. (2011). Regulation of lipopolysaccharide-induced translation of
887 tumor necrosis factor-alpha by the toll-like receptor 4 adaptor protein TRAM. J. Innate
888 Immun. *3*, 437–446. 10.1159/000324833.

889 31. Dumitru, C.D., Ceci, J.D., Tsatsanis, C., Kontoyiannis, D., Stamatakis, K., Lin, J.-H.,
890 Patriotis, C., Jenkins, N.A., Copeland, N.G., Kollias, G., et al. (2000). TNF-α Induction
891 by LPS Is Regulated Posttranscriptionally via a Tpl2/ERK-Dependent Pathway. Cell
892 *103*, 1071–1083. 10.1016/S0092-8674(00)00210-5.

893 32. Drecktrah, D., Knodler, L.A., Ireland, R., and Steele-Mortimer, O. (2006). The
894 mechanism of Salmonella entry determines the vacuolar environment and intracellular
895 gene expression. Traffic *7*, 39–51. 10.1111/J.1600-0854.2005.00360.X.

896 33. Man, S.M., Hopkins, L.J., Nugent, E., Cox, S., Glück, I.M., Tourlomousis, P., Wright,
897 J.A., Cicuta, P., Monie, T.P., and Bryant, C.E. (2014). Inflammasome activation
898 causes dual recruitment of NLRC4 and NLRP3 to the same macromolecular complex.
899 Proc. Natl. Acad. Sci. *111*, 7403–7408. 10.1073/PNAS.1402911111.

900 34. Fink, S.L., and Cookson, B.T. (2007). Pyroptosis and host cell death responses during
901 Salmonella infection. Cell. Microbiol. *9*, 2562–2570. 10.1111/J.1462-
902 5822.2007.01036.X.

903 35. Ingolia, N.T., Ghaemmaghami, S., Newman, J.R.S., and Weissman, J.S. (2009).
904 Genome-wide analysis in vivo of translation with nucleotide resolution using ribosome

905 profiling. Science *324*, 218–223. 10.1126/SCIENCE.1168978.

906 36. Chung, B.Y., Hardcastle, T.J., Jones, J.D., Irigoyen, N., Firth, A.E., Baulcombe, D.C.,
907 and Brierley, I. (2015). The use of duplex-specific nuclease in ribosome profiling and a
908 user-friendly software package for Ribo-seq data analysis. RNA *21*, 1731.
909 10.1261/RNA.052548.115.

910 37. Vattem, K.M., and Wek, R.C. (2004). Reinitiation involving upstream ORFs regulates
911 ATF4 mRNA translation in mammalian cells. Proc. Natl. Acad. Sci. *101*, 11269–
912 11274. 10.1073/pnas.0400541101.

913 38. Landmann, R., Knopf, H.P., Link, S., Sansano, S., Schumann, R., and Zimmerli, W.
914 (1996). Human monocyte CD14 is upregulated by lipopolysaccharide. Infect. Immun.
915 *64*, 1762–1769. 10.1128/IAI.64.5.1762-1769.1996.

916 39. Yang, H., Li, Q., Stroup, E.K., Wang, S., and Ji, Z. (2024). Widespread stable
917 noncanonical peptides identified by integrated analyses of ribosome profiling and
918 ORF features. Nat. Commun. 2024 151 *15*, 1–18. 10.1038/s41467-024-46240-9.

919 40. Bryant, C. (2021). Inflammasome activation by Salmonella. Curr. Opin. Microbiol. *64*,
920 27–32. 10.1016/j.mib.2021.09.004.

921 41. Qu, Y., Misaghi, S., Newton, K., Maltzman, A., Izrael-Tomasevic, A., Arnott, D., and
922 Dixit, V.M. (2016). NLRP3 recruitment by NLRC4 during Salmonella infection. J. Exp.
923 Med. *213*, 877–885. 10.1084/JEM.20132234.

924 42. Li, P., Allen, H., Banerjee, S., Franklin, S., Herzog, L., Johnston, C., McDowell, J.,
925 Paskind, M., Rodman, L., Salfeld, J., et al. (1995). Mice deficient in IL-1 beta-
926 converting enzyme are defective in production of mature IL-1 beta and resistant to
927 endotoxic shock. Cell *80*, 401–411. 10.1016/0092-8674(95)90490-5.

928 43. Hersh, D., Monack, D.M., Smith, M.R., Ghori, N., Falkow, S., and Zychlinsky, A.
929 (1999). The Salmonella invasin SipB induces macrophage apoptosis by binding to
930 caspase-1. Proc. Natl. Acad. Sci. *96*, 2396–2401. 10.1073/pnas.96.5.2396.

931 44. Cook, P., Tötemeyer, S., Stevenson, C., Fitzgerald, K.A., Yamamoto, M., Akira, S.,
932 Maskell, D.J., and Bryant, C.E. (2007). Salmonella-induced SipB-independent cell
933 death requires Toll-like receptor-4 signalling via the adapter proteins Tram and Trif.
934 Immunology *122*, 222. 10.1111/J.1365-2567.2007.02631.X.

935 45. Reyes Ruiz, V.M., Ramirez, J., Naseer, N., Palacio, N.M., Siddarthan, I.J., Yan, B.M.,
936 Boyer, M.A., Pensinger, D.A., Sauer, J.-D., and Shin, S. (2017). Broad detection of
937 bacterial type III secretion system and flagellin proteins by the human NAIP/NLRC4

938 inflammasome. Proc. Natl. Acad. Sci. *114*, 13242–13247. 10.1073/pnas.1710433114.

939 46. Mariathasan, S., Newton, K., Monack, D.M., Vucic, D., French, D.M., Lee, W.P.,
940 Roose-Girma, M., Erickson, S., and Dixit, V.M. (2004). Differential activation of the
941 inflammasome by caspase-1 adaptors ASC and Ipaf. Nature *430*, 213–218.
942 10.1038/nature02664.

943 47. Martin-Sanchez, F., Diamond, C., Zeitler, M., Gomez, A.I., Baroja-Mazo, A., Bagnall,
944 J., Spiller, D., White, M., Daniels, M.J.D., Mortellaro, A., et al. (2016). Inflammasome-
945 dependent IL-1β release depends upon membrane permeabilisation. Cell Death
946 Differ. *23*, 1219–1231. 10.1038/cdd.2015.176.

947 48. Lau, L.F., and Nathans, D. (1987). Expression of a set of growth-related immediate
948 early genes in BALB/c 3T3 cells: coordinate regulation with c-fos or c-myc. Proc. Natl.
949 Acad. Sci. *84*, 1182–1186. 10.1073/PNAS.84.5.1182.

950 49. McMahon, S.B., and Monroe, J.G. (1996). The role of early growth response gene 1
951 (egr-1) in regulation of the immune response. J. Leukoc. Biol. *60*, 159–166.
952 10.1002/JLB.60.2.159.

953 50. Bahrami, S., and Drabløs, F. (2016). Gene regulation in the immediate-early response
954 process. Adv. Biol. Regul. *62*, 37–49. 10.1016/J.JBIOR.2016.05.001.

955 51. Hamers, A.A.J., van Dam, L., Teixeira Duarte, J.M., Vos, M., Marinković, G., van Tiel,
956 C.M., Meijer, S.L., van Stalborch, A.-M., Huveneers, S., te Velde, A.A., et al. (2015).
957 Deficiency of nuclear receptor Nur77 aggravates mouse experimental colitis by
958 increased NFκB activity in macrophages. PLoS One *10*, e0133598.
959 10.1371/journal.pone.0133598.

960 52. Li, L., Liu, Y., Chen, H., Li, F., Wu, J., Zhang, H., He, J., Xing, Y., Chen, Y., Wang, W.,
961 et al. (2015). Impeding the interaction between Nur77 and p38 reduces LPS-induced
962 inflammation. Nat. Chem. Biol. *11*, 339–346. 10.1038/nchembio.1788.

963 53. Partyka, J., Henkel, M., Campfield, B.T., and 14, P.A. (2020). A Novel Role for the
964 Nuclear Receptor, NR4A1, in Klebsiella pneumoniae Lung Infection. bioRxiv,
965 2020.09.03.282475. 10.1101/2020.09.03.282475.

966 54. Thiel, G., and Cibelli, G. (2002). Regulation of life and death by the zinc finger
967 transcription factor Egr-1. J. Cell. Physiol. *193*, 287–292. 10.1002/jcp.10178.

968 55. Chbicheb, S., Yao, X., Rodeau, J.-L., Salamone, S., Boisbrun, M., Thiel, G., Spohn,
969 D., Grillier-Vuissoz, I., Chapleur, Y., Flament, S., et al. (2011). EGR1 expression: A
970 calcium and ERK1/2 mediated PPARγ-independent event involved in the

971 antiproliferative effect of 15-deoxy-Δ12,14-prostaglandin J2 and thiazolidinediones in
972 breast cancer cells. Biochem. Pharmacol. *81*, 1087–1097. 10.1016/j.bcp.2011.02.006.

973 56. Banerji, R., and Saroj, S.D. (2021). Early growth response 1 (EGR1) activation in
974 initial stages of host–pathogen interactions. Mol. Biol. Rep. *48*, 2935–2943.
975 10.1007/s11033-021-06305-0.

976 57. Trizzino, M., Zucco, A., Deliard, S., Wang, F., Barbieri, E., Veglia, F., Gabrilovich, D.,
977 and Gardini, A. (2021). EGR1 is a gatekeeper of inflammatory enhancers in human
978 macrophages. Sci. Adv. *7*. 10.1126/sciadv.aaz8836.

979 58. Kimura, T.E., Duggirala, A., Hindmarch, C.C.T., Hewer, R.C., Cui, M.Z., Newby, A.C.,
980 and Bond, M. (2014). Inhibition of Egr1 expression underlies the anti-mitogenic effects
981 of cAMP in vascular smooth muscle cells. J. Mol. Cell. Cardiol. *72*, 9–19.
982 10.1016/j.yjmcc.2014.02.001.

983 59. Sukhatme, V.P., Cao, X., Chang, L.C., Tsai-Morris, C.H., Stamenkovich, D., Ferreira,
984 P.C.P., Cohen, D.R., Edwards, S.A., Shows, T.B., Curran, T., et al. (1988). A zinc
985 finger-encoding gene coregulated with c-fos during growth and differentiation, and
986 after cellular depolarization. Cell *53*, 37–43. 10.1016/0092-8674(88)90485-0.

987 60. de Grado, M., Rosenberger, C.M., Gauthier, A., Vallance, B.A., and Finlay, B.B.
988 (2001). Enteropathogenic Escherichia coli infection induces expression of the early
989 growth response factor by activating mitogen-activated protein kinase cascades in
990 epithelial cells. Infect. Immun. *69*, 6217–6224. 10.1128/IAI.69.10.6217-6224.2001.

991 61. Shin, H., and Cornelis, G.R. (2007). Type III secretion translocation pores of Yersinia
992 enterocolitica trigger maturation and release of pro-inflammatory IL-1β. Cell. Microbiol.
993 *9*, 2893–2902. 10.1111/j.1462-5822.2007.01004.x.

994 62. Keates, S., Keates, A.C., Nath, S., Peek, R.M., and Kelly, C.P. (2005).
995 Transactivation of the epidermal growth factor receptor by cag+ Helicobacter pylori
996 induces upregulation of the early growth response gene Egr-1 in gastric epithelial
997 cells. Gut *54*, 1363–1369. 10.1136/gut.2005.066977.

998 63. Radics, J., Königsmaier, L., and Marlovits, T.C. (2013). Structure of a pathogenic type
999 3 secretion system in action. Nat. Struct. Mol. Biol. 2013 211 *21*, 82–87.
1000 10.1038/nsmb.2722.

1001 64. Kudryashev, M., Diepold, A., Amstutz, M., Armitage, J.P., Stahlberg, H., and Cornelis,
1002 G.R. (2015). Yersinia enterocolitica type III secretion injectisomes form regularly
1003 spaced clusters, which incorporate new machines upon activation. Mol. Microbiol. *95*,
1004 875–884. 10.1111/MMI.12908/SUPPINFO.

1005 65. Eriksson, S., Lucchini, S., Thompson, A., Rhen, M., and Hinton, J.C.D. (2003).
1006 Unravelling the biology of macrophage infection by gene expression profiling of
1007 intracellular Salmonella enterica. Mol. Microbiol. *47*, 103–118. 10.1046/j.1365-
1008 2958.2003.03313.x.

1009 66. Srikumar, S., Kröger, C., Hébrard, M., Colgan, A., Owen, S. V., Sivasankaran, S.K.,
1010 Cameron, A.D.S., Hokamp, K., and Hinton, J.C.D. (2015). RNA-seq brings new
1011 insights to the intra-macrophage transcriptome of Salmonella Typhimurium. PLOS
1012 Pathog. *11*, e1005262. 10.1371/journal.ppat.1005262.

1013 67. Chakraborty, S., Mizusaki, H., and Kenney, L.J. (2015). A FRET-based DNA
1014 biosensor tracks OmpR-dependent acidification of Salmonella during macrophage
1015 infection. PLOS Biol. *13*, e1002116. 10.1371/journal.pbio.1002116.

1016 68. Pérez-Morales, D., Banda, M.M., Chau, N.Y.E., Salgado, H., Martínez-Flores, I.,
1017 Ibarra, J.A., Ilyas, B., Coombes, B.K., and Bustamante, V.H. (2017). The
1018 transcriptional regulator SsrB is involved in a molecular switch controlling virulence
1019 lifestyles of Salmonella. PLOS Pathog. *13*, e1006497. 10.1371/journal.ppat.1006497.

1020 69. Brown, N.F., Rogers, L.D., Sanderson, K.L., Gouw, J.W., Hartland, E.L., and Foster,
1021 L.J. (2014). A horizontally acquired transcription factor coordinates Salmonella
1022 adaptations to host microenvironments. MBio *5*, 1727–1741. 10.1128/mBio.01727-14.

1023 70. Bryant, C. (2021). Inflammasome activation by Salmonella. Curr. Opin. Microbiol. *64*,
1024 27–32. 10.1016/j.mib.2021.09.004.

1025 71. Advani, V.M., and Ivanov, P. (2019). Translational control under stress: reshaping the
1026 translatome. BioEssays *41*, e1900009. 10.1002/BIES.201900009.

1027 72. Hoang, H.D., Neault, S., Pelin, A., and Alain, T. (2021). Emerging translation
1028 strategies during virus–host interaction. Wiley Interdiscip. Rev. RNA *12*.
1029 10.1002/WRNA.1619.

1030 73. Yan, S.F., Fujita, T., Lu, J., Okada, K., Shan Zou, Y., Mackman, N., Pinsky, D.J., and
1031 Stern, D.M. (2000). Egr-1, a master switch coordinating upregulation of divergent
1032 gene families underlying ischemic stress. Nat. Med. *6*, 1355–1361. 10.1038/82168.

1033 74. Hughes, S.A., Lin, M., Weir, A., Huang, B., Xiong, L., Chua, N.K., Pang, J.,
1034 Santavanond, J.P., Tixeira, R., Doerflinger, M., et al. (2023). Caspase-8-driven
1035 apoptotic and pyroptotic crosstalk causes cell death and I-1β release in X-linked
1036 inhibitor of apoptosis (XIAP) deficiency. EMBO J. *42*. 10.15252/embj.2021110468.

1037 75. Wang, Y., and Kanneganti, T.-D. (2021). From pyroptosis, apoptosis and necroptosis

1038 to PANoptosis: A mechanistic compendium of programmed cell death pathways.
1039 Comput. Struct. Biotechnol. J. *19*, 4641–4657. 10.1016/j.csbj.2021.07.038.

1040 76. Ponde, N.O., Lortal, L., Tsavou, A., Hepworth, O.W., Wickramasinghe, D.N., Ho, J.,
1041 Richardson, J.P., Moyes, D.L., Gaffen, S.L., and Naglik, J.R. (2022). Receptor-kinase
1042 EGFR-MAPK adaptor proteins mediate the epithelial response to Candida albicans
1043 via the cytolytic peptide toxin, candidalysin. J. Biol. Chem. *298*.
1044 10.1016/j.jbc.2022.102419.

1045 77. De Nardo, D., Kalvakolanu, D. V., and Latz, E. (2018). Immortalization of Murine Bone
1046 Marrow-Derived Macrophages. In Methods in molecular biology (Clifton, N.J.)
1047 (Humana Press Inc.), pp. 35–49. 10.1007/978-1-4939-7837-3_4.

1048 78. Irigoyen, N., Firth, A.E., Jones, J.D., Chung, B.Y.W., Siddell, S.G., and Brierley, I.
1049 (2016). High-resolution analysis of Coronavirus gene expression by RNA sequencing
1050 and ribosome profiling. PLOS Pathog. *12*, e1005473. 10.1371/journal.ppat.1005473.

1051 79. Chung, B.Y.W., Deery, M.J., Groen, A.J., Howard, J., and Baulcombe, D.C. (2017).
1052 Endogenous miRNA in the green alga Chlamydomonas regulates gene expression
1053 through CDS-targeting. Nat. Plants 2017 310 *3*, 787–794. 10.1038/s41477-017-0024-
1054 6.

1055 80. Chung, B.Y.W., Balcerowicz, M., Di Antonio, M., Jaeger, K.E., Geng, F., Franaszek,
1056 K., Marriott, P., Brierley, I., Firth, A.E., and Wigge, P.A. (2020). An RNA thermoswitch
1057 regulates daytime growth in Arabidopsis. Nat. Plants 2020 65 *6*, 522–532.
1058 10.1038/s41477-020-0633-3.

1059 81. Xiao, Z., Zou, Q., Liu, Y., and Yang, X. (2016). Genome-wide assessment of
1060 differential translations with ribosome profiling data. Nat. Commun. *7*.
1061 10.1038/ncomms11194.

1062 82. Robinson, M.D., McCarthy, D.J., and Smyth, G.K. (2010). edgeR: a Bioconductor
1063 package for differential expression analysis of digital gene expression data.
1064 Bioinformatics *26*, 139–140. 10.1093/BIOINFORMATICS/BTP616.

1065 83. Peterson, H., Kolberg, L., Raudvere, U., Kuzmin, I., and Vilo, J. (2020). gprofiler2 - an
1066 R package for gene list functional enrichment analysis and namespace conversion
1067 toolset g:Profiler. F1000Research *9*, 709. 10.12688/f1000research.24956.2.

1068 84. Wise, D. (2019). Understanding antigen processing in chickens using genome editing
1069 technology. 10.17863/CAM.40666.

1070 85. Amann, E., Ochs, B., and Abel, K.J. (1988). Tightly regulated tac promoter vectors

1071 useful for the expression of unfused and fused proteins in Escherichia coli. Gene *69*,
1072 301–315. 10.1016/0378-1119(88)90440-4.

1073 86. Bryant, O.J., Dhillon, P., Hughes, C., and Fraser, G.M. (2022). Recognition of discrete
1074 export signals in early flagellar subunits during bacterial type III secretion. Elife *11*.
1075 10.7554/eLife.66264.

1076

Figure 1

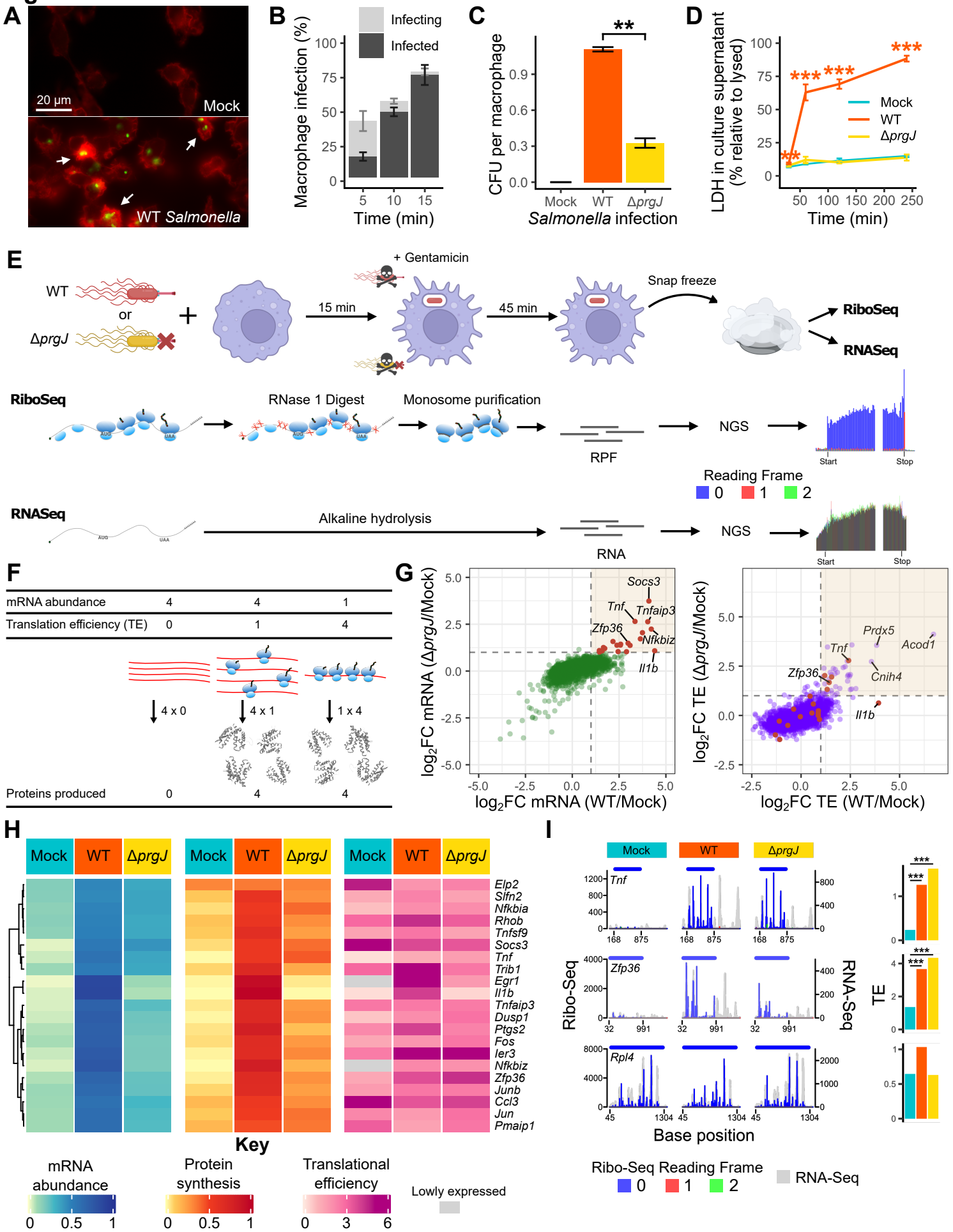
A
20 µm
Mock
WT Salmonella
B
Infecting
Infected
Macrophage infection (%)
Time (min)
C
CFU per macrophage
Mock
WT
ΔprgJ
Salmonella infection
D
LDH in culture supernatant (% relative to lysed)
Mock
WT
ΔprgJ
Time (min)
E
WT
or
ΔprgJ
+ Gentamicin
15 min
45 min
Snap freeze
RiboSeq
RNASeq
RNase 1 Digest
Monosome purification
RPF
NGS
Start
Stop
Reading Frame
0
1
2
Alkaline hydrolysis
RNA
F
mRNA abundance 4 4 1
Translation efficiency (TE) 0 1 4
4 x 0
4 x 1
1 x 4
Proteins produced 0 4 4
G
Socs3
Tnf
Tnfaip3
Zfp36
Nfkbiz
Il1b
log2FC mRNA (ΔprgJ/Mock)
log2FC mRNA (WT/Mock)
Prdx5
Acod1
Cnih4
log2FC TE (ΔprgJ/Mock)
log2FC TE (WT/Mock)
H
Mock
WT
ΔprgJ
Elp2
Slfn2
Nfkbia
Rhob
Tnfsf9
Socs3
Tnf
Trib1
Egr1
Il1b
Tnfaip3
Dusp1
Ptgs2
Fos
Ier3
Nfkbiz
Zfp36
Junb
Ccl3
Jun
Pmaip1
Key
mRNA abundance
Protein synthesis
Translational efficiency
Lowly expressed
I
Tnf
Zfp36
Rpl4
Ribo-Seq
RNA-Seq
TE
Base position
Ribo-Seq Reading Frame
RNA-Seq

Figure 1 Cont.

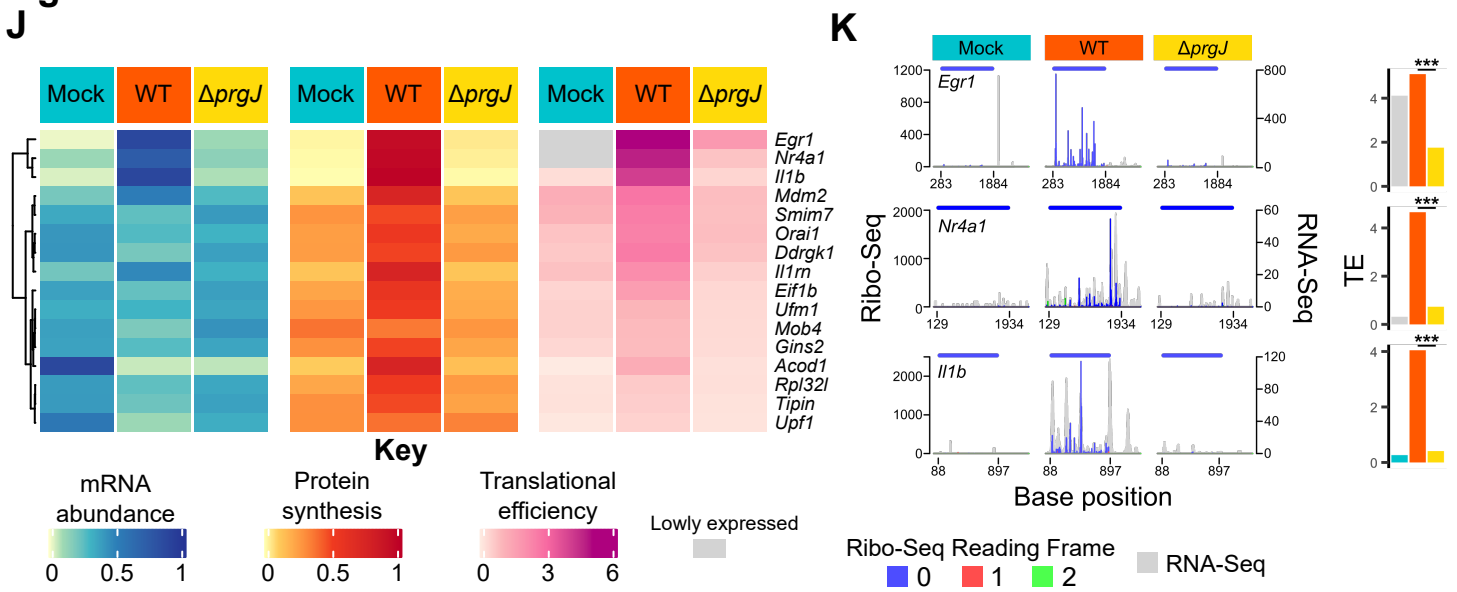

Figure 2

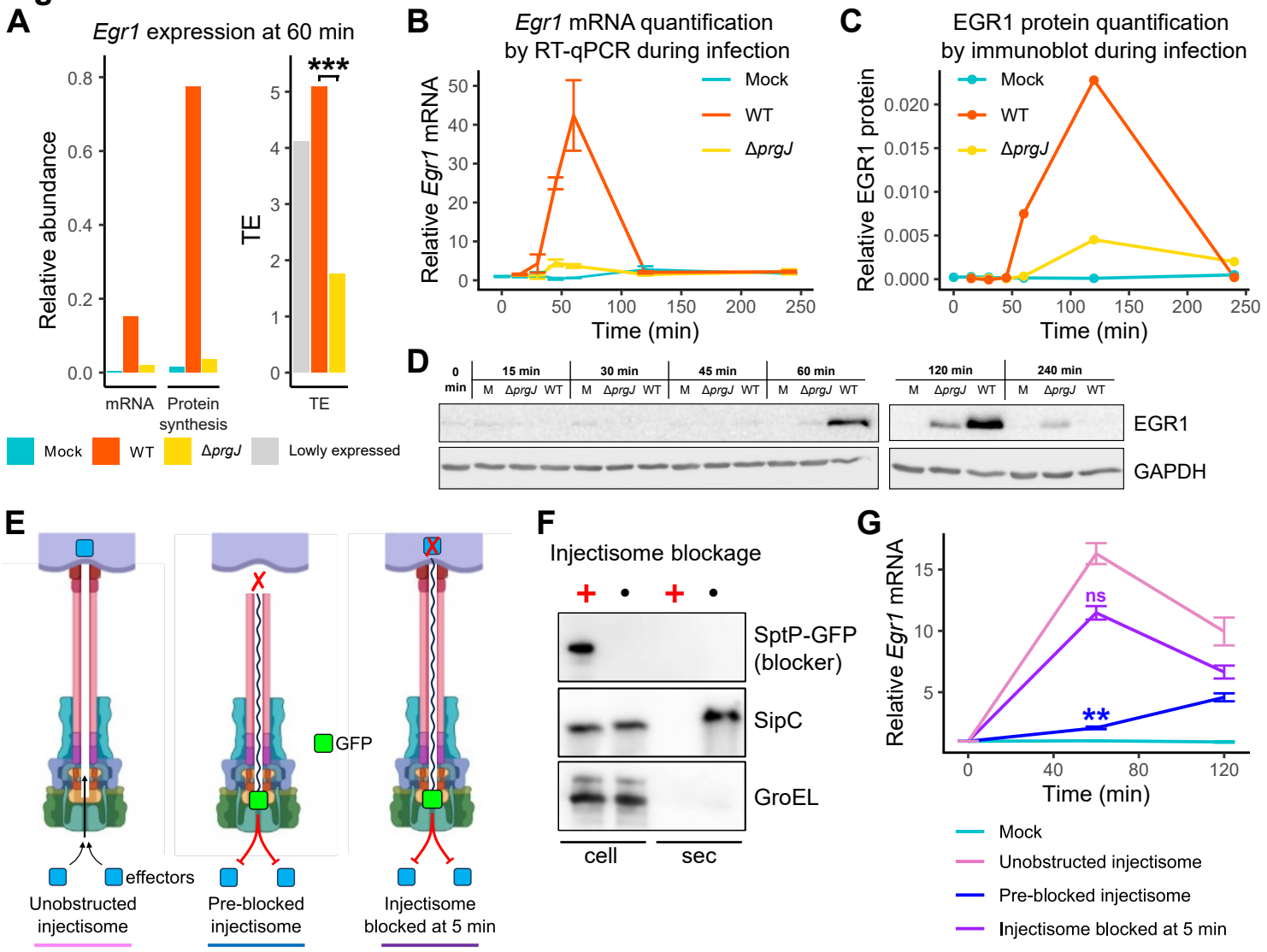
A
Egr1 expression at 60 min
Relative abundance
0.8
0.6
0.4
0.2
0.0
mRNA
Protein synthesis
TE
***
5
4
3
2
1
0
Mock
WT
ΔprgJ
Lowly expressed
B
Egr1 mRNA quantification by RT-qPCR during infection
Relative Egr1 mRNA
50
40
30
20
10
0
Mock
WT
ΔprgJ
0
50
100
150
200
250
Time (min)
C
EGR1 protein quantification by immunoblot during infection
Relative EGR1 protein
0.020
0.015
0.010
0.005
0.000
Mock
WT
ΔprgJ
0
50
100
150
200
250
Time (min)
D
0 min
15 min
30 min
45 min
60 min
120 min
240 min
M
ΔprgJ
WT
EGR1
GAPDH
E
effectors
GFP
Unobstructed injectisome
Pre-blocked injectisome
Injectisome blocked at 5 min
F
Injectisome blockage
+
•
SptP-GFP (blocker)
SipC
GroEL
cell
sec
G
Relative Egr1 mRNA
15
10
5
ns
**
0
40
80
120
Time (min)
Mock
Unobstructed injectisome
Pre-blocked injectisome
Injectisome blocked at 5 min

Figure 2 Cont.

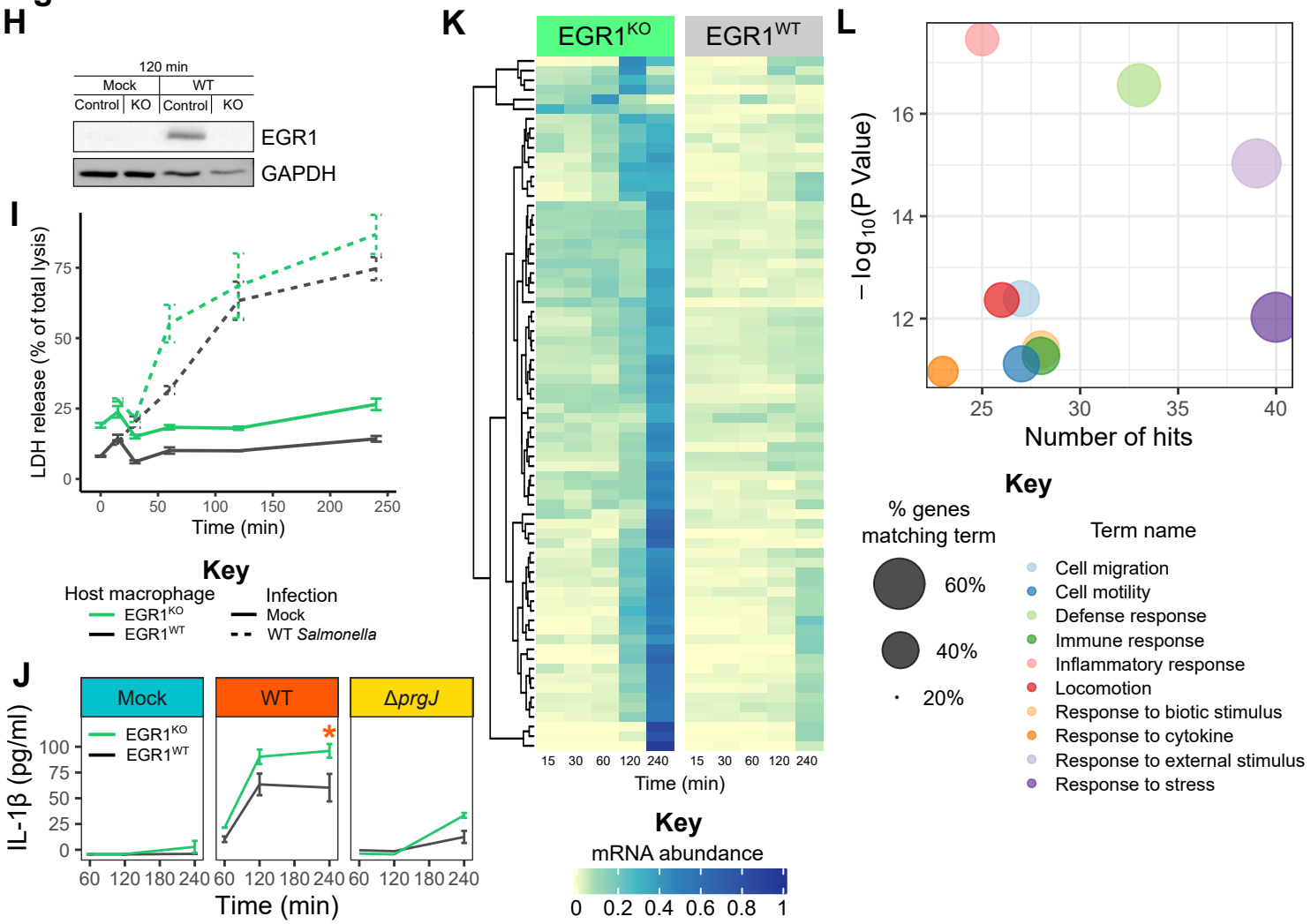

Figure 3

A

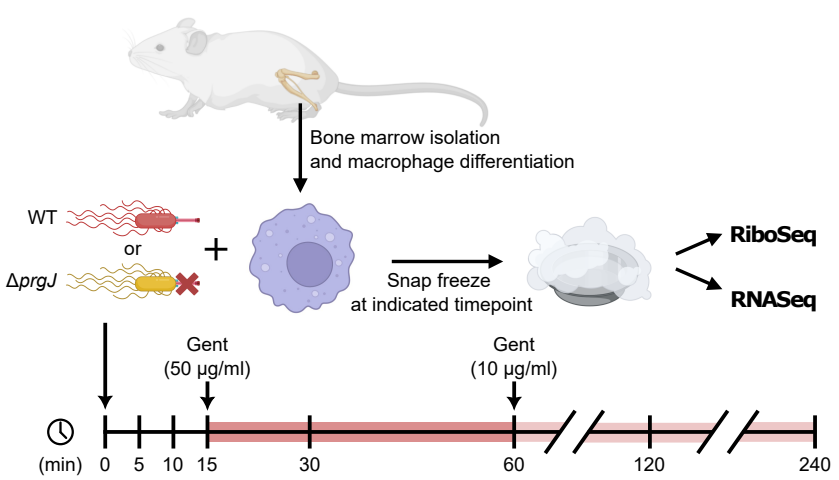
Bone marrow isolation
and macrophage differentiation
WT
or
ΔprgJ
Snap freeze
at indicated timepoint
RiboSeq
RNASeq
Gent
(50 µg/ml)
Gent
(10 µg/ml)
(min)
0
5
10
15
30
60
120
240

B

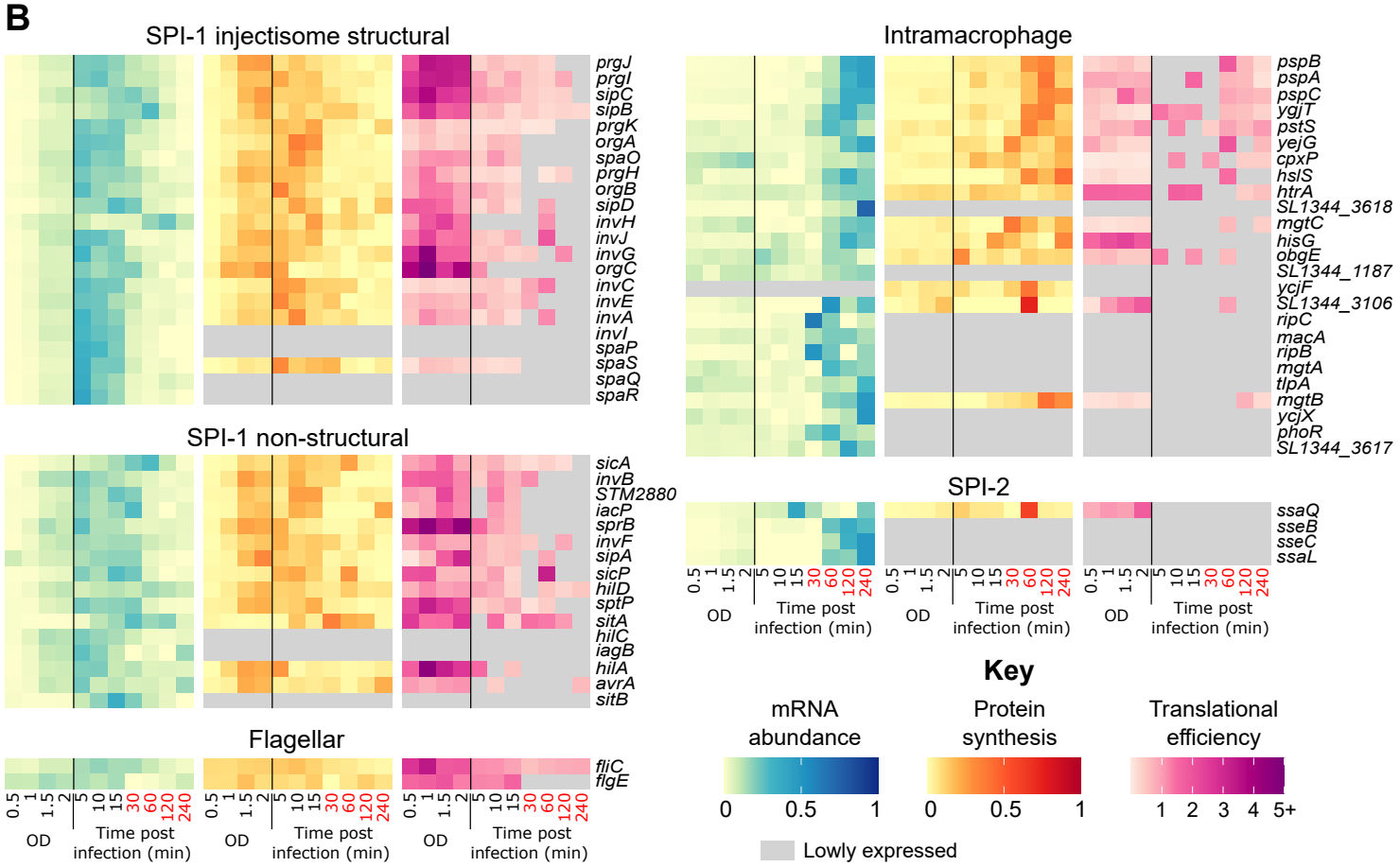
SPI-1 injectisome structural
prgJ
prgI
sipC
sipB
prgK
orgA
spaO
prgH
orgB
sipD
invH
invJ
invG
orgC
invC
invE
invA
invI
spaP
spaS
spaQ
spaR
SPI-1 non-structural
sicA
invB
STM2880
iacP
sprB
invF
sipA
sicP
hilD
sptP
sitA
hilC
iagB
hilA
avrA
sitB
Flagellar
fliC
flgE
Intramacrophage
pspB
pspA
pspC
ygjT
pstS
yejG
cpxP
hslS
htrA
SL1344_3618
mgtC
hisG
obgE
SL1344_1187
ycjF
SL1344_3106
ripC
macA
ripB
mgtA
tlpA
mgtB
ycjX
phoR
SL1344_3617
SPI-2
ssaQ
sseB
sseC
ssaL
0.5
1
1.5
2
5
10
15
30
60
120
240
OD
Time post
infection (min)
Key
mRNA
abundance
Protein
synthesis
Translational
efficiency
0
0.5
1
1
2
3
4
5+
Lowly expressed

Figure 3 Cont.

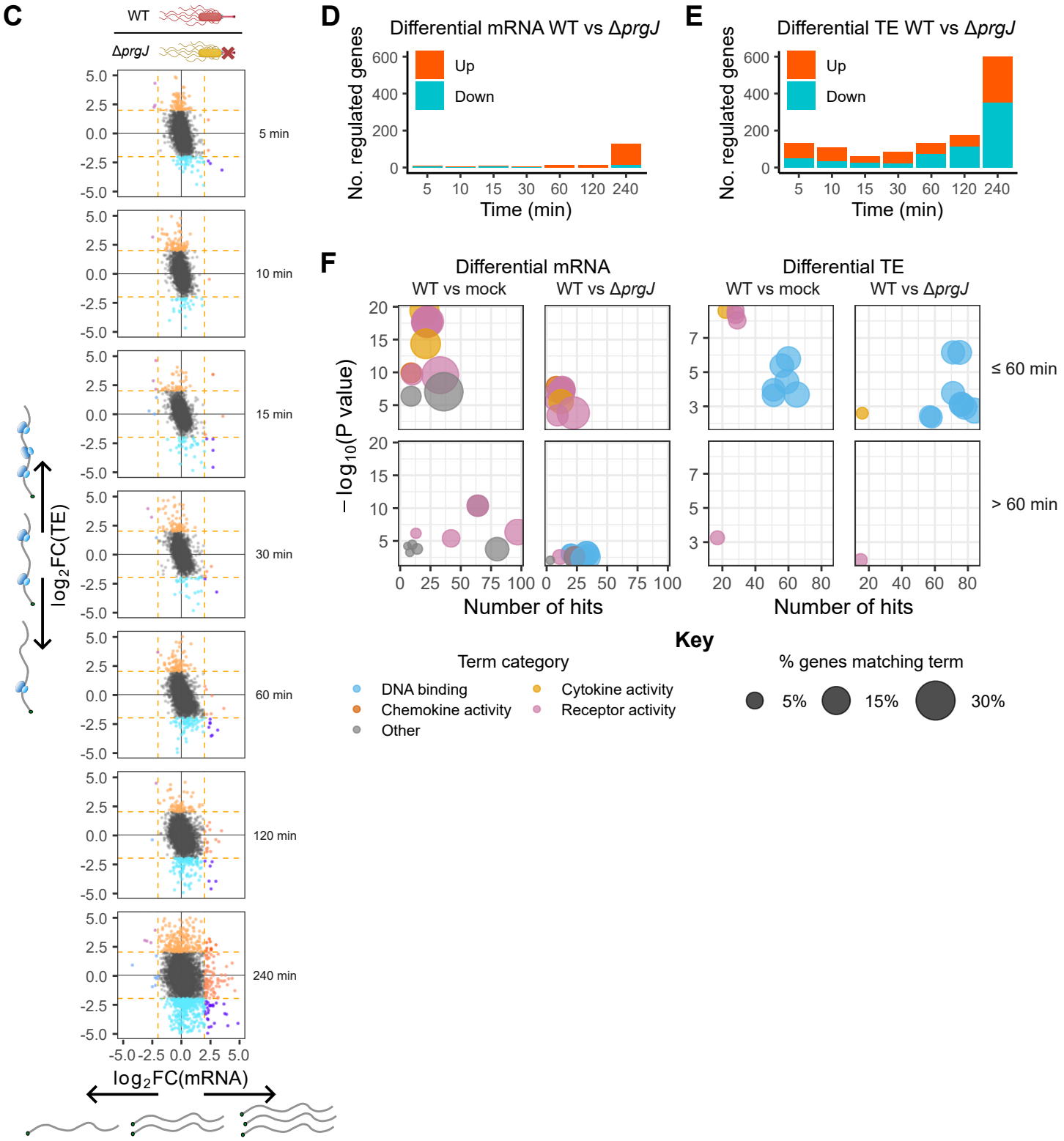

Figure 4

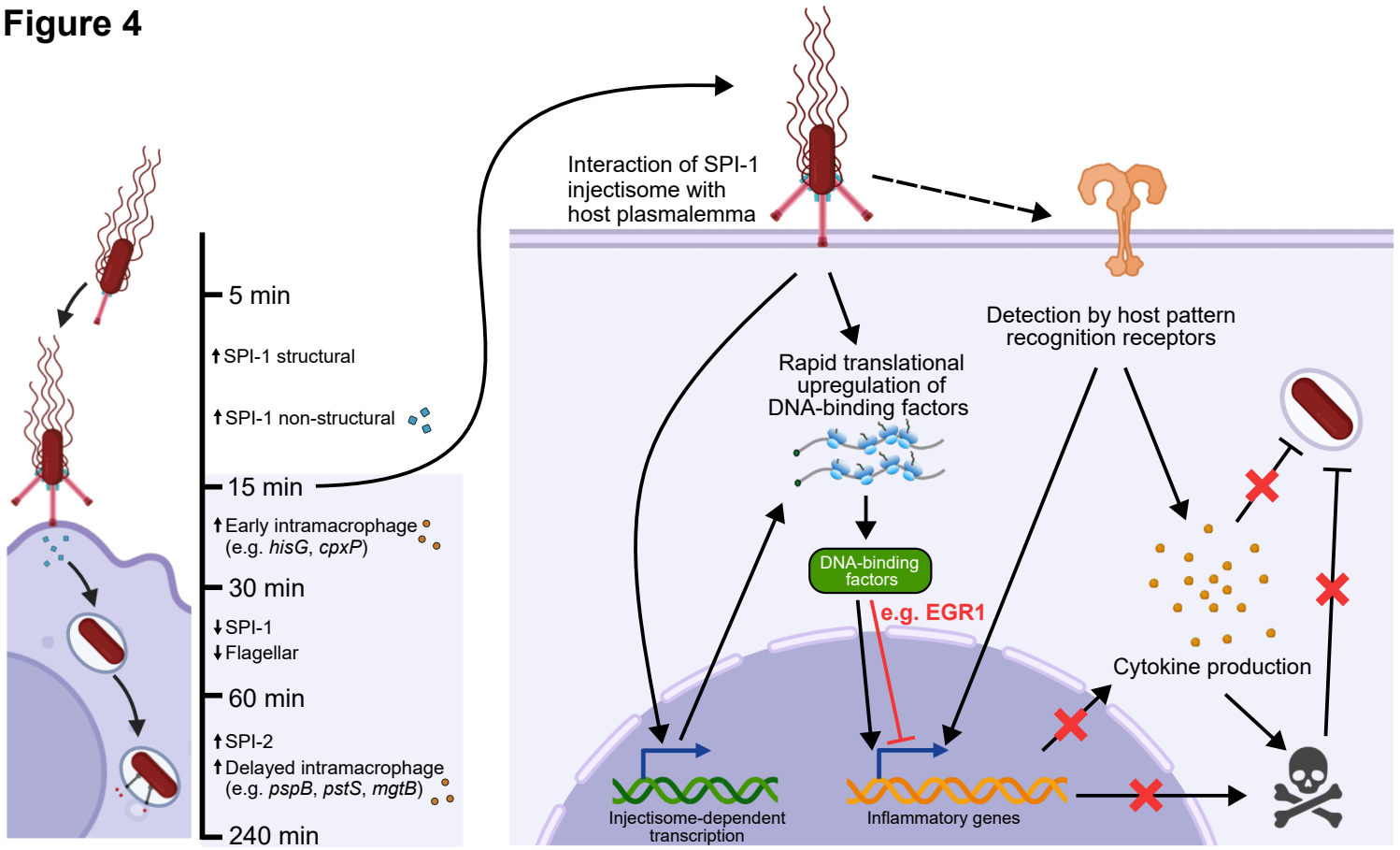
5 min
SPI-1 structural
SPI-1 non-structural
15 min
Early intramacrophage
(e.g. *hisG*, *cpxP*)
30 min
SPI-1
Flagellar
60 min
SPI-2
Delayed intramacrophage
(e.g. *pspB*, *pstS*, *mgtB*)
240 min
Interaction of SPI-1
injectisome with
host plasmalemma
Detection by host pattern
recognition receptors
Rapid translational
upregulation of
DNA-binding factors
DNA-binding
factors
e.g. EGR1
Cytokine production
Injectisome-dependent
transcription
Inflammatory genes